A SPECTROSCOPIC INVESTIGATION OF THE ρ PUPPIS STARS

A Thesis
by
Courtney Elizabeth McGahee

Submitted to the Graduate School
Appalachian State University
in partial fulfillment of the requirements for the degree of
Master of Science

May 2010
Department of Physics and Astronomy

A SPECTROSCOPIC INVESTIGATION OF THE ρ PUPPIS STARS

A Thesis
by
Courtney Elizabeth McGahee

APPROVED BY:

Richard O. Gray
Chairperson, Thesis Committee

Daniel B. Caton
Member, Thesis Committee

Adrian N. Daw
Member, Thesis Committee

Leon Ginsberg
Interim Chairperson, Physics and Astronomy

Edelma D. Huntley
Dean, Research and Graduate Studies

ABSTRACT

A SPECTROSCOPIC INVESTIGATION OF THE ρ PUPPIS STARS
May 2010

Courtney Elizabeth McGahee, B.Sc., Appalachian State University

M.Sc., Appalachian State University, Boone

Chairperson: Richard Gray

The ρ Puppis stars are mid F-type stars that show peculiar chemical abundance patterns similar to those of the hotter Am stars. This means that they typically exhibit overabundances of iron-peak elements like Fe and Ni as well as s- and r-process elements such as Sr and Eu, but show underabundances of other elements like He and Ca. There are currently two hypotheses that may explain these peculiar chemical abundances. One hypothesis suggests that these stars are evolving Am stars in a short-lived phase that occurs between the re-establishment of convection and the consequent erasure of the chemical peculiarities. The second hypothesis requires that these stars have acquired their peculiar abundance patterns in a fashion similar to the Barium dwarf stars. More specifically, it is suspected that they may have gained the s-process element enhancements via mass transfer from a once Asymptotic Giant-Branch companion star, now turned white dwarf.

This thesis details my efforts to investigate the ρ Puppis stars with regard to these two hypotheses, so that we may understand these stars and their

significance in terms of stellar evolution. To carry out this investigation a spectral classification survey was conducted to increase the number of ρ Puppis stars currently known. A chemical-abundance analysis of selected ρ Puppis stars was also carried out to give us insight into the chemical make-up of their atmospheres. Because this study showed that there are consistent enhancements of Eu, an r-process element, in the atmospheres of the ρ Puppis stars, I conclude that it is more likely that the ρ Puppis stars are evolved Am stars. I will also consider the relationship between the extreme/late Fm stars and the ρ Puppis stars.

ACKNOWLEDGMENTS

First and foremost, I would like to acknowledge Dr. Richard O. Gray, without whose guidance, support and endless encouragement, this project would not have been possible.

I also wish to express the most sincere thanks to Dr. Elizabeth Griffin, for her hospitality, friendship and tireless assistance in this project.

Thank you to all those at the Dominion Astrophysical Observatory of the Herzberg Institute of Astrophysics in Victoria, B.C., Canada for their unlimited support, friendly reception and accommodation.

I would also like to acknowledge Sigma Xi for research funding through their Grants-In-Aid of Research Program, without which this research would not have been possible.

Finally, my heartfelt thanks to friends and family for the support they have shown throughout the years.

Contents

Chapter 1

Introduction

The ρ Puppis stars are stars that show similar abundance patterns to those of the metallic-line A-type stars, or Am stars, but that possess effective temperatures of the cooler, mid F-type stars. ρ Puppis stars, like Am stars, show overabundances of iron-peak elements such as Fe and Ni as well as s- and r-process elements such as Sr and Eu. However they tend to show underabundances of other elements like He and Ca. It was once thought that Am stars should not exist below a certain lower effective-temperature limit; however, ρ Puppis stars have effective temperatures cooler than this limit and yet still show the abundance pattern of Am stars.

Two hypotheses have been developed to attempt to explain the existence of this peculiar abundance pattern present in the ρ Puppis stars. The first hypothesis suggests that the ρ Puppis stars are in fact evolving Am stars, caught in a short-lived phase between the re-establishment of convection and the subsequent erasure of the chemical-abundance peculiarities. The second hypothesis suggests that these stars are not related to the Am stars, but rather to the Barium dwarfs, a group of stars that has a similar abundance pattern to the ρ Puppis stars, but acquires those abun-

dances via mass transfer from an Asymptotic Giant-Branch (AGB) companion star, now turned white dwarf.

This thesis is an investigation of the ρ Puppis stars with respect to these two hypotheses so that we may determine which of these two physical mechanisms can be producing the unexplained chemical peculiarities. To carry out this investigation I first conducted a spectroscopic classification survey to increase the number of ρ Puppis stars currently known. I then carried out a chemical-abundance analysis of selected ρ Puppis stars that allowed a more detailed look at the chemical make-up of the atmospheres of these stars.

Because ρ Puppis stars may be related to the somewhat hotter Am stars, it is essential to understand the past research on the Am stars. The Am stars are a subclass of the spectroscopically classified A-type stars and are characterized by overabundances of iron-peak elements, such as Fe, Ni and Cr, heavy metals, such as Sr, and rare earths in their atmospheres. At the same time, they show underabundances of other elements like He and Ca. It should be noted that Am and Fm stars share the same characteristics and that the A/F distinction is due to an effective-temperature classification based on the hydrogen-line type, which will be discussed in the Classifications section.

The most widely accepted theory that explains the Am abundance pattern was presented by Michaud (1970) to explain the peculiar abundance patterns of Ap stars, another subgroup of A-type stars that show enhancements and deficiencies of particular elements. He proposed that diffusive chemical separation is the mechanism causing the abundance anomalies observed in Ap stars because it would allow certain elements to be pushed up to the top of a star's atmosphere via radiation pressure, while allowing other elements to sink. Chemical separation occurs because for some elements,

the outward radiative acceleration ($g_{\rm rad}$) can exceed the inward gravitational acceleration (g), causing these elements to rise to the top of a star's atmosphere. For other elements, $g_{\rm rad} < g$, causing these elements to sink. The distinction between which elements rise and which ones sink arises because the average direction of motion for photons emitted from a star's core is radially outward, and because the momentum of any particular photon is inversely proportional to the photon's wavelength. Therefore, atoms of elements with many absorption lines in the ultraviolet will gain more outward momentum from absorbed photons causing $g_{\rm rad}$ to be greater than g, whereas for atoms of elements with few lines in the ultraviolet, g will remain dominant.

Michaud (1970) used chemical separation to explain the abundance anomalies of Ap stars, but stated that for chemical separation to have an effect on the observed abundance pattern, the atmosphere of the Ap star must be stable, otherwise, mixing would erase the effects of chemical separation. He suggested that Ap stars did in fact have stable enough atmospheres for chemical separation to be effective, and this was due in part to the fact that most Ap stars are known to be slow rotators, but he also pointed out that the strength of the magnetic fields associated with these stars may be the key to their stable atmospheres. Michaud suggested that the magnetic fields of Ap stars may affect the stability of the atmosphere by reducing convection and meridional circulation (a circulation that is induced by rotation) as well as directly inhibiting the diffusion of ions via the Lorentz force. The latter would explain why only certain elements are enhanced in Ap stars.

Watson (1970), building on Michaud's work, attempted to apply the diffusion and chemical separation theory to the Am stars. Watson (1971) agreed with Michaud that diffusion and chemical separation would in fact give abundance anomalies that were in good agreement with observations and attributed this to the fact that Ap stars

have both low rotational velocities and strong magnetic fields which help to induce stable atmospheres in which chemical separation can operate. He suggested, however, that while Am stars possess low rotational velocities, they have weak magnetic fields and that, in fact, Am stars tend to have quite turbulent atmospheres. The lack of a strong magnetic field in Am stars also helps to explain why most metals in Am stars are enhanced, in contrast to the Ap stars in which only certain metals are enhanced.

To compensate for the atmospheric turbulence present in Am stars, Watson (1971) proposed that the chemical separation in Am stars occurs in a region at the base of the outer convective zone, which coincides with the He I ionization zone. Both Smith (1971) and Charbonneau (1993) continued research in this area and agreed with Watson, that the chemical separation explaining the abundance anomalies of Am stars would only require a stable zone in which to operate. That stable radiative zone is achieved in part by the fact that almost all Am stars are slow rotators, as was pointed out by Slettebak (1954, 1955) who showed a systematic association between Am stars and low rotational velocities. Unlike Ap stars which seem to have gained their low rotational velocities due to magnetic braking, Am stars appear to have achieved their slow rotation by being in a close binary system. This widely accepted theory can be inferred from two findings: 1) Abt (1961) showed that most Am stars are in binary systems, and 2) Kreiken (1935) demonstrated that binary system components can have slower rotational velocities due in part to tidal interactions. However, Kreiken pointed out that gravity is not the only factor, and that other factors should also be considered.

It has been theorized that "normal" A-type stars would show the Am abundance pattern if it were not for meridional circulation induced by rapid rotation. It has also been pointed out that normal A-type stars achieve some of their "normalcy" via Delta

Scuti pulsations, driven by He ionization, which help in mixing a star's atmosphere. Charbonneau (1993) demonstrated that in Am stars, chemical separation dominates over meridional circulation, allowing He to sink and most metals to rise. This leads to the disappearance of the He ionization zone in Am stars, and thus the disappearance of the Delta Scuti pulsations in Am stars, which in turn allows chemical separation to dominate in the region all the way up to the base of the "superficial hydrogen convection zone" (Charbonneau 1993). Figure 1.1 summarizes Charbonneau's depiction of the placement of the stable radiative zone in both normal A-type and Am stars. The lack of mixing induced by slow rotation and the absence of He ionization serves to preserve the abundance pattern created by diffusion, by allowing the separation of elements to remain relatively undisturbed.

Because He ionization is dependent on the effective temperature ($T_{\rm eff}$) of a star, so too is the dormancy of He ionization zone. Smith (1973) showed that the Am abundance pattern can only be maintained above a certain lower limit of the stellar $T_{\rm eff}$. He related this lower temperature limit to the rotational velocity ($V_{\rm rot}$) of the star showing that there exists a critical rotational velocity ($V_{\rm crit}$) which is a function of the effective temperature. He stated that the "incidence (of Fm stars) decreases rapidly coolward of a sharp peak at type A6-7 because a rotational velocity 'barrier' imposes itself such that only stars with $V_{\rm rot} < V_{\rm crit}$ ($T_{\rm eff}$) can contain metallicism." He demonstrated that $V_{\rm crit}$ decreases with $T_{\rm eff}$ until it approaches 0 km/s at F2 and that his findings are "in qualitative agreement with Stromgren's (1963) discovery that the occurrence of large m_1 indices suddenly ceases for types later than F1 $(b-y) = .21$ mag." Smith added that in stars cooler than F2, He ionization zones become more extensive causing convection in the once stable radiative zone, which should aid in erasing any peculiar abundance patterns that had developed.

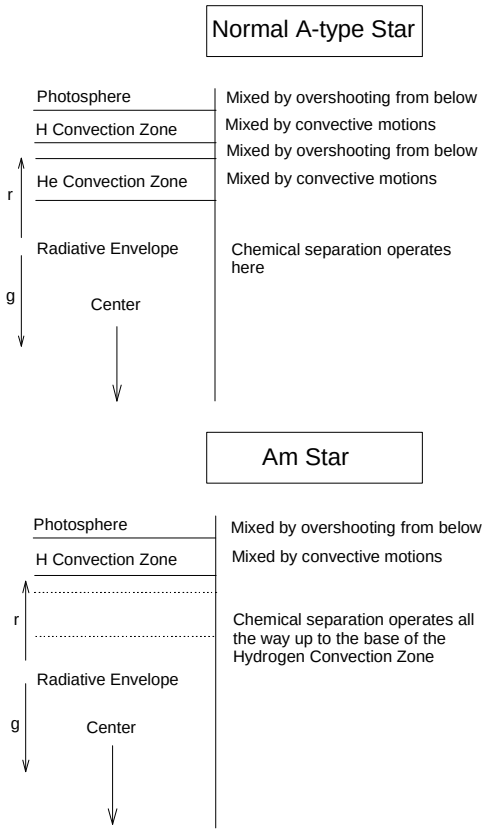

Figure 1.1 A figure depicting the placement of the radiative envelope in both a normal A-type star and an Am star, adapted from Charbonneau (1993).

Gray & Garrison (1989) reported, however, that there does exist a small subclass of Fm stars that are cooler than spectral type F2. They discovered this group while working to reclassify the δ Delphini stars, a now defunct class of stars originally defined as metallic-line stars in which the difference in the Ca II-K line type and the

metallic-line type was small. Gray & Garrison's work to reclassify the δ Delphini stars showed that the majority of these stars fell into four groups. They found that a number of the stars appeared to be relatively normal, and proposed that they were classified as peculiar because they possessed narrow spectral lines that were caused by low rotational velocities. A second group appeared to be relatively normal, but evolved, F-type stars with marginal enhancements of the metallic-line spectrum. The third and perhaps largest group are now known as the proto-Am stars, which are Am stars in which the discrepancy between the metallic-line and the Ca II K-line type is small (less than 5 spectral subclasses). The fourth group, according to Gray & Corbally (2009), was the only group to "appear to form a distinct and interesting class of stars."

This fourth, distinct group consisted of only four stars: ρ Pup, θ Gru, HD 103877 and τ UMa. Gray & Garrison labeled this group "ρ Puppis" after the brightest in the class. ρ Puppis stars appear quite similar to the Am/Fm stars in that they share the same abundance anomalies including overabundances of Fe and Sr, and underabundances of Ca and He. Supporting an Am relation, Gray & Corbally (2009) stated that ρ Puppis stars appear to be late Am stars because they exhibit a feature known as the "Anomalous Luminosity Effect," a feature commonly found among Am stars having to do with wavelength-dependent luminosity classifications. This characteristic will be covered in more detail in the Classifications section.

Gray & Corbally point out, however, that the existence of these ρ Puppis stars is fascinating because "their hydrogen line types are F5, remarkably late for Am stars," and their exhibition of the Anomalous Luminosity Effect is extreme, meaning they present wavelength-related discrepancies in their luminosity classifications that are larger than those presented in most Am stars. Considering Gray & Corbally's

findings, the existence of ρ Puppis stars poses a theoretical problem since they are stars that show the same chemical-abundance peculiarities as Am stars, yet they lie outside of the pre-determined boundaries for which it was thought possible for stars to show metallicism.

In addition, Gray & Corbally (2009) pointed out that ρ Puppis itself is known to undergo large-amplitude δ Scuti pulsations. It is quite perplexing that ρ Puppis exhibits δ Scuti pulsations on two counts. The first is that this star presumably lacks the driving mechanism (He ionization) for these pulsations to take place, and yet they are present. The second is that despite these pulsations, we still see the Am abundance anomalies that should be erased due to mixing induced by the pulsations. The fact that ρ Puppis is experiencing δ Scuti pulsations may prove consistent with the theory that ρ Puppis stars are simply evolved Am stars in that (1) it indicates that either the He ionization zone remained intact or has been re-established in order to drive these pulsations (Kurtz *et al.* 1976) and (2) it was predicted by Smith (1973) that Am stars that had cooled enough to regain their He ionization zones and that had crossed the rotational velocity barrier for which metallicism can exist, would be favored to exhibit δ Scuti type pulsations. Gray & Corbally (2009) suggest, in light of the points above, that ρ Puppis stars may in fact be Am stars in a short-lived phase between the re-establishment of their convective zones and the consequent erasure of their chemical peculiarities.

There is, however, a second hypothesis, put forward by Gray, to explain the existence of ρ Puppis stars. It suggests that the ρ Puppis stars are related to another group of chemically peculiar F-type stars known as the Barium dwarf stars. Barium dwarfs show chemical peculiarities somewhat similar to Am stars, but have, it is believed, gained these peculiarities via mass transfer from a former Asymptotic Giant

Branch (AGB) companion star, now turned white dwarf (McClure 1983; North & Lanz 1991). The abundance patterns of Ba dwarfs differ from those of the Am stars in that the Ba dwarfs have spectral types between F5 and early G, and that they tend to only show enhancements of Sr and Ba as opposed to an overall metal enhancement like in the Am stars.

This hypothesis that suggests a relationship between ρ Puppis stars and Barium dwarfs seems plausible when one considers the fact that originally, the prevailing hypothesis explaining the chemical abundance pattern of Am stars also invoked mass transfer. Warner (1965) showed that the overabundances of heavy elements in Barium stars was explained satisfactorily by the s-process (slow neutron capture process) of nucleosynthesis. Until about 1970, Am stars were compared to the Barium stars because they presented similar enhancements of Ba and Sr. In addition, hypotheses were proposed that suggested that slowly rotating Am stars must have undergone mass transfer from a more massive companion star which has since evolved into a white dwarf, in order to achieve their low rotational velocities (van den Heuvel 1968). The mass-transfer hypothesis, however, was quite quickly discarded with regard to Am stars on a number of counts.

The mass-transfer hypothesis required that either the Am star itself or its binary companion be in a late stage of evolution in order to undergo s-process nucleosynthesis. Smith (1971) pointed out that the discovery of Am stars in very young clusters by Conti & Strom (1968), Conti & van den Heuvel (1970), Garrison (1967) and Glaspey (1971) was inconsistent with this idea. He also stated that it would be difficult to imagine a combination of α capture, e- (electron capture), r- (rapid neutron capture) and s- (slow neutron capture) processes occurring in an unevolved Am star without it leading to widely disparate abundances, and that it is very unlikely that the e-process

necessary to explain the iron-peak abundances would be operative in the Am stars in view of the extreme conditions required. Smith also dispelled the idea that a chemical separation during the protocloud phase was responsible because in this case, it would be unlikely that different abundance patterns would appear on the surfaces of the two companion stars of a binary system, as was also reported by Conti (1969). He therefore concluded that it was unlikely that nucleosynthesis was responsible for the Am phenomenon.

Despite the dissociation of Am stars and the mass-transfer hypothesis, we still consider mass transfer as a possible explanation of the ρ Puppis conundrum because the ρ Puppis stars do in fact show similar abundances of the s-process elements Ba and Sr, to Barium dwarfs, and their placement in the Am scheme is questionable because of their cool effective temperatures. The best way to determine which of these two proposed hypotheses explains the chemical-abundance anomalies of ρ Puppis stars is to conduct a detailed chemical-abundance analysis.

Barium dwarfs obtain their chemical abundances via the s-process which causes enhancements of Sr and Ba. Am stars tend to show enhancements of Sr and Ba as well, however the hypothesis that Am stars gain these particular enhancements via the s-process is inconsistent with other characteristics of the Am stars. ρ Puppis stars do in fact show enhancements of both Sr and Ba (as will be demonstrated), but in this study I will pay close attention to the abundance of Eu, as it is largely an r-process element. If Eu is found to be consistently overabundant, it will help to confirm the evolved Am star hypothesis, whereas if we find solar abundances of Eu in ρ Puppis stars it will point to the mass-transfer hypothesis.

Chapter 2

Selection of Candidate ρ Puppis Stars

The goal of this thesis is to elucidate the nature of the ρ Puppis stars. Because only five stars are currently classified as members of the ρ Puppis class, the first task was to discover more members of the class. I accomplished this with two observing strategies.

The first strategy involved a closer look at the previously classified δ Delphini stars from which Gray & Garrison (1989) found the first ρ Puppis stars. Around 1970, Nancy Houk embarked on a large-scale project to systematically reclassify the HD (Henry Draper) catalog with two dimensions (temperature and luminosity classifications) using the MK standard stars for comparison. This ended up as a multi-volume publication and to date only the southern hemisphere has been completed. Using Volumes 4 (Houk & Smith-Moore 1988) and 5 (Houk & Swift 1999) which surveyed the sky from -26° to +5° declination, I selected all of the stars that Houk classified as δ Delphini as candidate stars for classification-resolution observations.

I was limited to Volumes 4 and 5 of this work, because spectroscopic observations carried out at Appalachian State University's Dark Sky Observatory (DSO) can only be made down to -25° declination. The δ Delphini target list proved to be too short (only 100 stars), and did not provide me with the number of candidate stars I desired. To increase the size of our ρ Puppis candidate list, I employed a second strategy in which I selected about 300 stars from the Mermilliod photometric catalog (Mermilliod, Mermilliod & Hauck 1997) using Strömgren photometry. The Strömgren photometric system employs four medium-bandwidth filters in the u (ultraviolet), v (visible), b (blue) and y (yellow) and is designed for the purpose of classifying stars. Magnitudes measured through these filters may be combined into photometric indices that can be used to calculate temperature $(b-y)$, the metallicity of a star (m_1) and an index that measures the Balmer jump (c_1).

The m_1 and c_1 indices are defined as follows:

$$m_1 = (v-b) - (b-y)$$

$$c_1 = (u-v) - (v-b)$$

To compensate for interstellar reddening, reddening-free versions of the indices may be defined:

$$[m_1] = m_1 + 0.32(b-y)$$

$$[c_1] = c_1 - 0.2(b-y)$$

I chose to plot the stars in the Mermilliod catalog in the $[m_1]$, $[c_1]$ plane as presented in Figure 2.1. Am, Fm and ρ Puppis stars have high values of m_1 as they exhibit enhancements of their metallic-line spectrum. In F-type stars, the c_1 index is sensitive to surface gravity with a negative correlation, e.g., a giant star will have a larger Balmer jump than a dwarf star, corresponding to a lower gravity. It became

evident when I plotted the four known ρ Puppis stars with the Mermilliod catalog stars, that the ρ Puppis stars were grouped together, and possessed higher $[m_1]$ values than most of the stars in the Mermilliod catalog, as anticipated. Using the ρ Puppis indices as guidelines, I selected ρ Puppis candidates with similar $[m_1]$ and $[c_1]$ values as indicated by the red box in Figure 2.1.

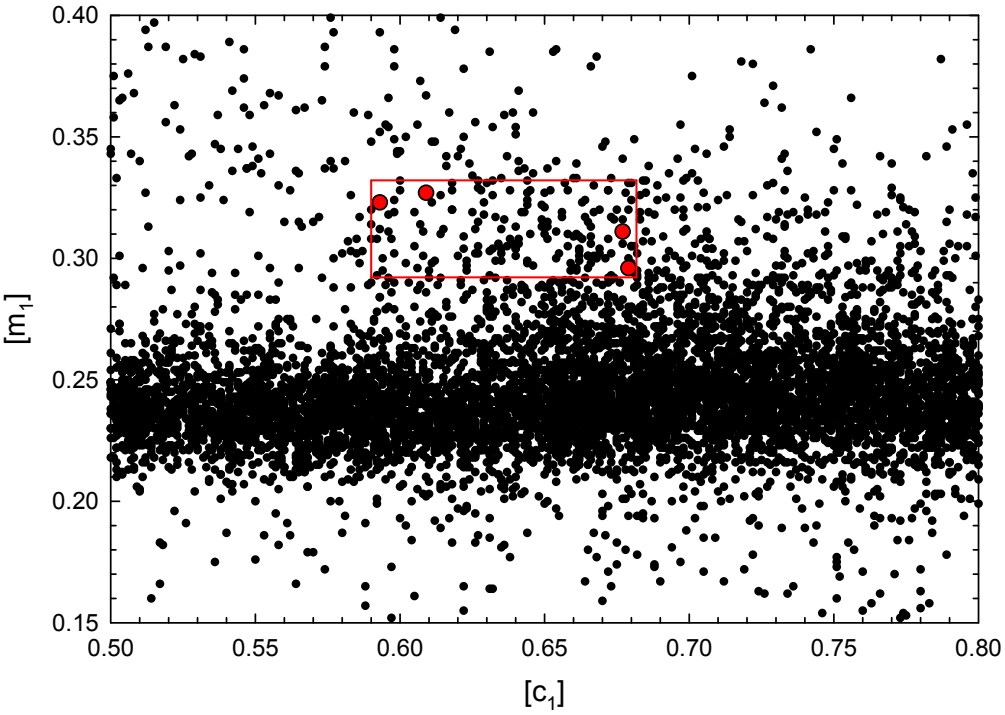

Figure 2.1 A plot of the Mermilliod Catalog stars according to their uvby photometric indices $[m_1]$ and $[c_1]$. The red box indicates the boundaries of $[m_1]$ and $[c_1]$ in which my ρ Puppis candidates were contained.

Chapter 3

Observations

Observations for this thesis were carried out with both low- and high-resolution spectrographs. Low-resolution (classification-resolution) observations were obtained so that I could classify the stars on the ρ Puppis candidate list. The low-resolution spectra are of sufficient resolution to classify the spectra visually. Using the low-resolution spectra for classification purposes is a more efficient use of observing time because exposure times needed to attain acceptable signal to noise ratios (S/N) for low-resolution spectra are much shorter than those required for high-resolution spectra. High-resolution spectra, however, were necessary to carry out the abundance analysis because the programs used to conduct the analysis required a high resolution in order to measure equivalent widths of spectral lines, as will be detailed in the Abundance Analysis section.

The resolution for a spectrograph can be expressed in two ways. The first way is to express the resolution in terms of the full width at half maximum (FWHM) of the "line-spread function." This line spread function, a characteristic of the spectrograph itself, is usually approximately a Gaussian, and represents the output of a spectro-

graph when monochromatic light is incident on the entrance aperture, or slit. The FWHM is usually expressed in angstroms (Å) or nanometers (nm). The second way to express the resolution is as

$$R = \lambda/\Delta\lambda$$

where $\Delta\lambda$ = FWHM of the line-spread function and λ is the central wavelength at which the observations are made.

3.1 Classification-Resolution Observations

Classification-resolution spectra of the ρ Puppis candidates were obtained on the 32-inch DFM Engineering telescope of Appalachian State University's Dark Sky Observatory, located in the Blue Ridge mountains of North Carolina. The Gray-Miller Cassegrain spectrograph was used for these observations. The detector employed was a back-illuminated 1024 X 1024 Tektronix CCD used in the MPP mode. The 600 and 1200 grooves/mm gratings were utilized in conjunction with a 100-micron wide slit to produce 3.6 and 1.8 Å/2 pixel resolutions (R = 1300 and R = 2300) with spectral ranges of 3800-5600 and 3800-4600 Å respectively. Exposure times were calculated to achieve a signal to noise ratio (S/N) > 100. The observed spectra were reduced with standard methods including flat fielding, dark subtraction and bias removal. All reductions were carried out via IRAF[1]. The wavelength calibration was determined by using comparison spectra obtained with an Fe-Ar hollow-cathode lamp. The reduced spectra were rectified using an X Window System program, xmk22, written by Richard Gray (Gray & Corbally 2009).

[1]IRAF is distributed by the National Optical Astronomy Observatories, which are operated by the Association of Universities for Research in Astronomy, Inc., under cooperative agreement with the National Science Foundation.

3.2 High-Resolution Observations

Obtaining high-resolution spectra of selected ρ Puppis stars was necessary in order to carry out the chemical-abundance analysis. High-resolution spectra were obtained in three particular spectral regions carefully chosen to yield abundances of Fe, Ca, Si, Ti, Ba, Sr and Eu. At the invitation of Dr. Elizabeth Griffin, I applied for and was awarded multiple observing runs throughout 2008 and 2009 on the 1.2 meter telescope at the Dominion Astrophysical Observatory (DAO) of the Herzberg Institute of Astrophysics in Victoria, British Columbia, Canada. Funded by Sigma Xi's Grants-In-Aid of Research[2], I traveled to DAO for two 6-night long visiting observer runs, one in July 2008 and the other in October 2008. In addition, I was awarded a robotic observing run in November of the same year, however, Dr. Griffin graciously offered to perform the observations herself. In May 2009, I was awarded a fourth visiting observer run, funded by a NASA GALEX Space Telescope Grant[3], during which I was able to obtain spectra of both ρ Puppis stars and Barium dwarf stars.

Observations initially targeted a region in the red part of the spectrum, spanning 6100-6250 Å. Observations were made in this region in order to determine the abundances of Fe, Ca and Si. Figure 3.1 shows the spectrum of HD 103877 observed in this region, with Fe I, Ca I and Si I lines marked. Secondly, I focused on a region centered on the Hδ line, stretching between (and including) the two Sr II resonance lines at 4077 and 4215 Å. Figure 3.2 shows the Sr II and Eu II lines used to calculate the corresponding abundances for these stars. Lastly I focused on a region stretching between 4415-4558 Å which was used to determine the Ba and Ti abundances of these stars and also included the region of the spectrum associated with the Anomalous

[2]Sigma Xi, The Scientific Research Society, Research Triangle Park, N.C.

[3]NASA Grant NNX09AD64G

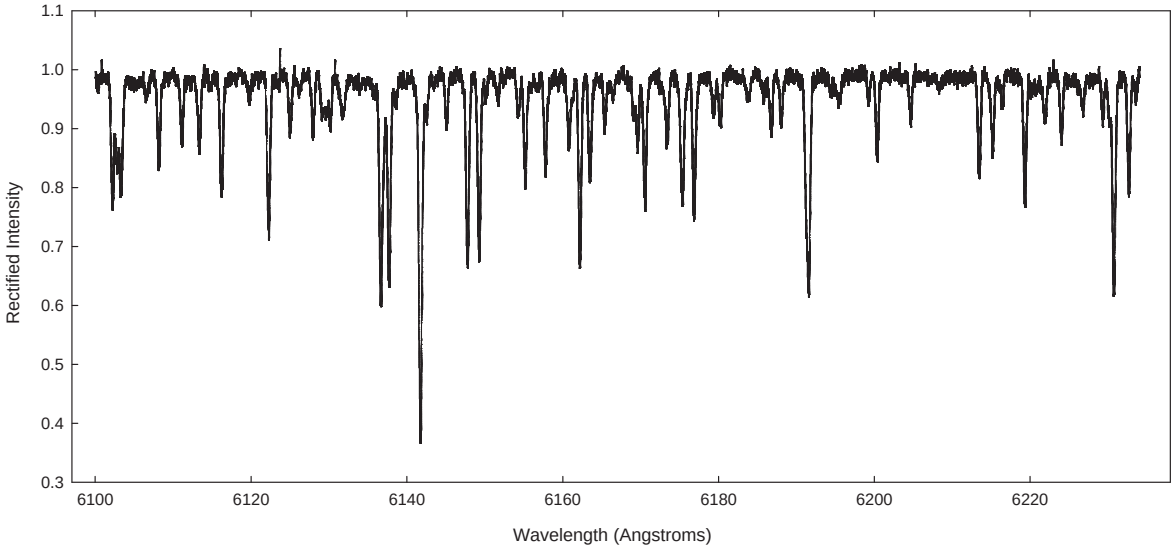

Figure 3.1 A high-resolution spectrum in the red obtained at DAO for HD 103877 with marked lines of Fe I, Ca I and Si I.

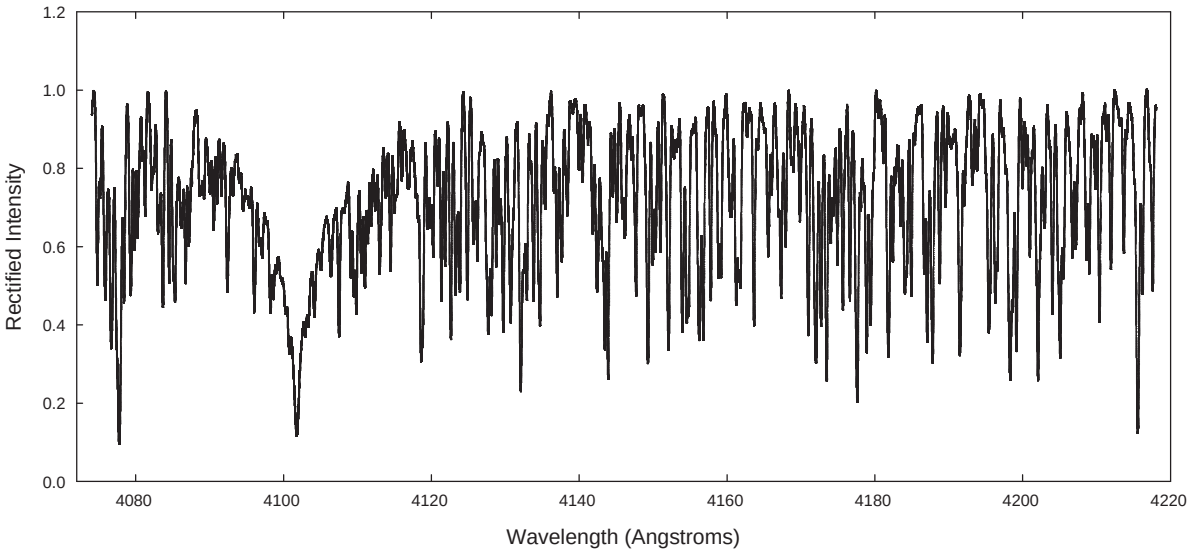

Figure 3.2 A high-resolution spectrum in the violet obtained at DAO for HD 103877 with marked lines of Sr II, Eu II and the Hδ line for reference.

Luminosity Effect. Figure 3.3 shows the DAO spectrum marked with Ti I and II lines as well as the Ba II line. Observations of a set of 18 stars classified as ρ Puppis by myself and Dr. Richard Gray, as well as two known ρ Puppis stars, HD 103877 and τ UMa, were obtained for at least one of the three regions of interest at DAO[4].

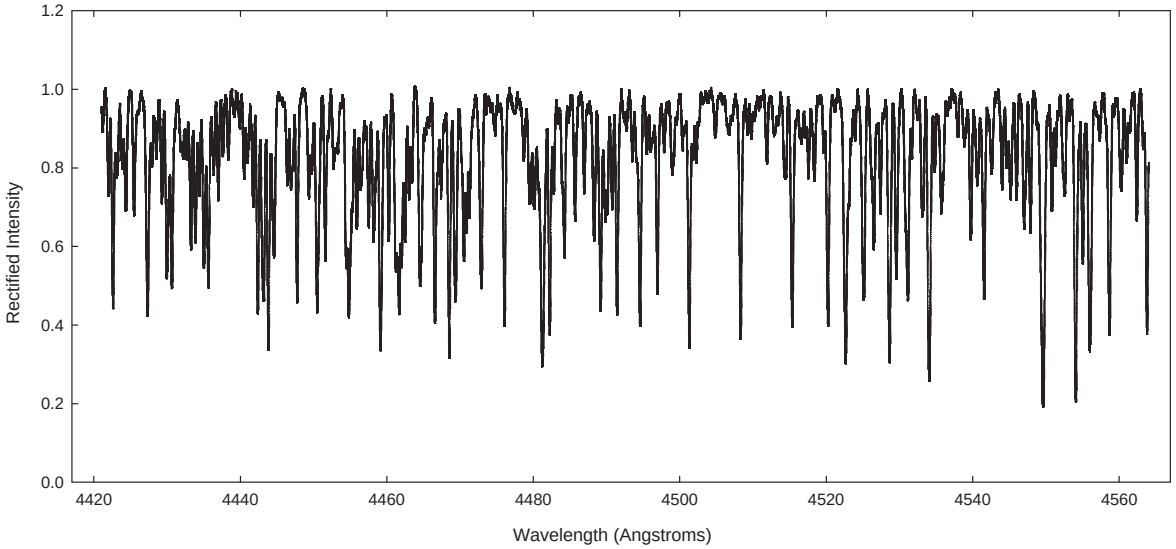

Figure 3.3 A high-resolution spectrum in the blue obtained at DAO for HD 103877 with marked lines of Ti I, Ti II and the the Ba II line at 4554 Å.

The 1.2 meter telescope and McKellar coudé spectrograph were employed in high-dispersion mode (96-inch camera, mosaic grating with 830 lines/mm, and a Richardson image slicer). The spectra have a dispersion near 2.4 Å/mm and cover a wavelength range of about 140 Å with a resolving power of $R = 85,000$ in the blue and $R = 30,000$ in the red. Comparison spectra of hollow-cathode discharge lamps (Fe/Ar for the blue region and Th/Ar for the red region) were used for wavelength calibration. These spectra were reduced with a semiautomatic IRAF-based pipeline operated by D. A. Bohlender. The reductions were performed by Elizabeth Griffin. I

[4]Guest investigator, Dominion Astrophysical Observatory, Herzberg Institute of Astrophysics, National Research Council of Canada.

then corrected the spectra for 3.5% scattered light before they were employed in the abundance analysis (Adelman *et al.* 2006; Gulliver, Hill & Adelman 1996).

Chapter 4

Classifications

The spectral classifications of the program stars observed at DSO were carried out on the MK system (Morgan, Keenan & Kellman 1943). Spectral types are two dimensional classifications determined by the temperature (or spectral) type and the luminosity type of a star. This typically results in a classification label consisting of spectral class denoted by a capital letter (O, B, A, F, G, K, M, L or T), followed by a subtype (0-9), and a luminosity type indicated by a Roman numeral (typically I-V).

The OBAFGKMLT sequence refers to a temperature sequence, O representing the hottest temperature class and T representing the coolest. This sequence generates the term "O-type," "A-type," etc. to describe a star. Approximate surface temperature ranges associated with each spectral type are given for dwarf stars of that type in Table 4.1. Each of these temperature ranges is further divided into ten smaller ranges denoted by 0-9, 0 corresponding to the hottest subtype of a temperature class and 9 corresponding to the coolest. The luminosity class is correlated with the surface gravity of a star and gives us information on the evolutionary state. The different luminosity classes and their corresponding Roman numerals are given in Table 4.2.

Table 4.1 Effective temperature ranges of the major spectral type groups. Data derived from Gray & Corbally (2009).

Spectral Type	Surface Temperature Range
O	31,884- 44,852 K
B	10,700-29,000K
A	7,380-9,800K
F	6,010-7,250 K
G	5,350-5,900 K
K	4,130-5,280 K
M	2,544-3,759 K
L	1,329-2,409 K

Table 4.2 Luminosity types on the MK system and their meanings.

Luminosity Class	Evolutionary State
V	dwarf
IV	subgiant
III	giant
II	bright giant
Ib	supergiant
Ia	bright supergiant
0	hypergiant

A luminosity classification of V refers to a dwarf or main-sequence star while the rest of the labels refer to stars that have evolved off the main-sequence. It is important to note that it is common for a star to be labeled with an "intermediate" luminosity class by a classification such as III-IV. As an example of how this classification label is employed, our sun, classified as a G2 V, has a surface temperature of 5778 K, and is a main-sequence (dwarf) star, meaning that it generates energy by the fusion of hydrogen to helium.

The MK spectral classification system is an empirical scheme based on the comparison of unknowns with standard stars. This comparison is carried out visually using certain spectral criteria as aids. The MK system was first devised by Morgan, Keenan & Kellman (1943). It has been revised and refined since that time. The current state of this system is described in Gray & Corbally (2009).

In normal A-type stars, we can use the width and strength of the hydrogen Balmer lines to determine the temperature (or spectral) type, e.g., A5. The width of the Balmer lines increases with temperature in the early A-type stars, peaks around a temperature corresponding with spectral type A2, and then decreases with decreasing temperature. In addition, a strengthening of the Ca II K-line, as well as an overall strengthening of the metallic-line spectrum can be observed with decreasing temperature. Figure 4.1 shows how the hydrogen lines grow weaker from spectral type A3 to F0. It also shows a notable strengthening of both the Ca II K-line and the overall metallic-line spectrum with decreasing temperature.

The hydrogen lines, in addition to being temperature indicators, show a sensitivity to luminosity in the early A-type stars, however this sensitivity decreases as temperature decreases and is almost non-existent in the F-type stars. In the cooler or "later" A-type stars and in the F-type stars where the hydrogen lines are no longer

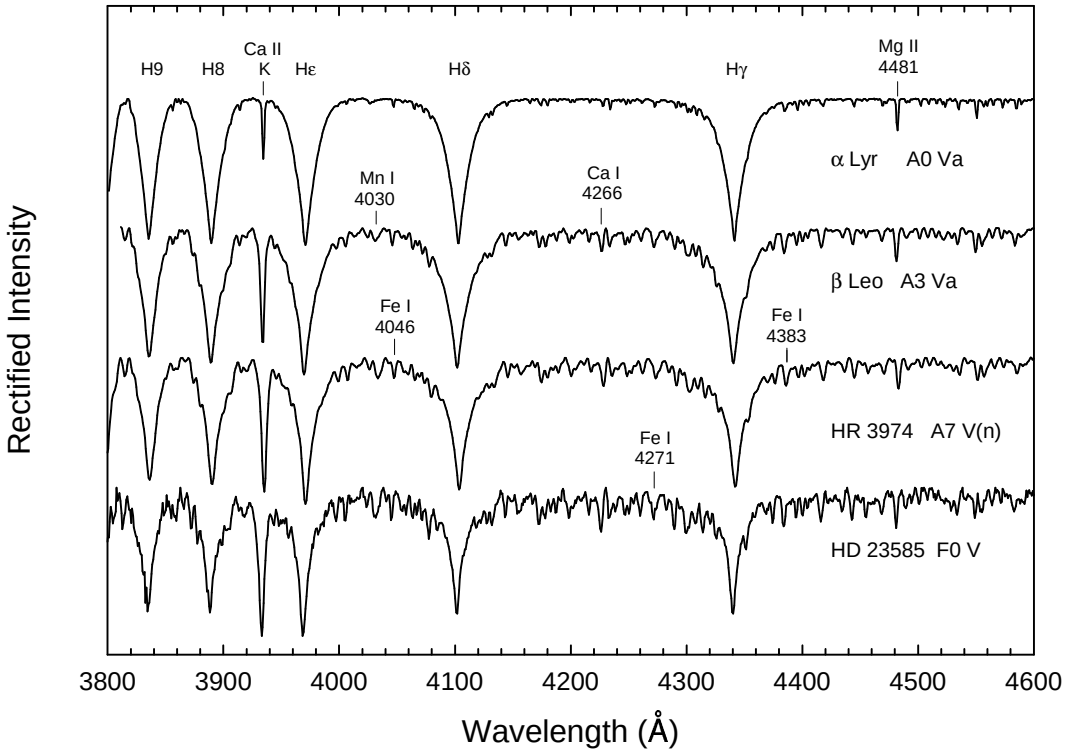

Figure 4.1 A demonstration of a temperature sequence of A-type stars. Note how the hydrogen lines weaken with a decrease in temperature, but how the Ca II K-line and the metals strengthen as temperature decreases.

usable in luminosity determination, certain lines of singly ionized Ti and Fe can be used, as they show an increase in strength with an increase in luminosity. There are two specific Fe II/Ti II features that are typically used in the determination of the luminosity classification. The first is a blend of Fe II and Ti II at $\lambda\lambda$4172-4179. The second is a "forest" (Gray & Corbally 2009) of Fe II and Ti II that lies between λ4395 and λ4600. In normal A- and F- type stars, these two features give consistent luminosity types.

Figure 4.2 shows a luminosity sequence for A7 stars, in which the sensitivity of the hydrogen lines to luminosity type is still prevalent. In addition we see that the sensi-

tivity of the Fe II and Ti II lines is also pronounced, from dwarf to bright supergiant. Figure 4.3 shows a decrease in the sensitivity of the hydrogen lines to luminosity in F0 stars, especially for the giant to supergiant luminosities. The sensitivity of the Fe II/Ti II lines and blends to luminosity however, is still prominent.

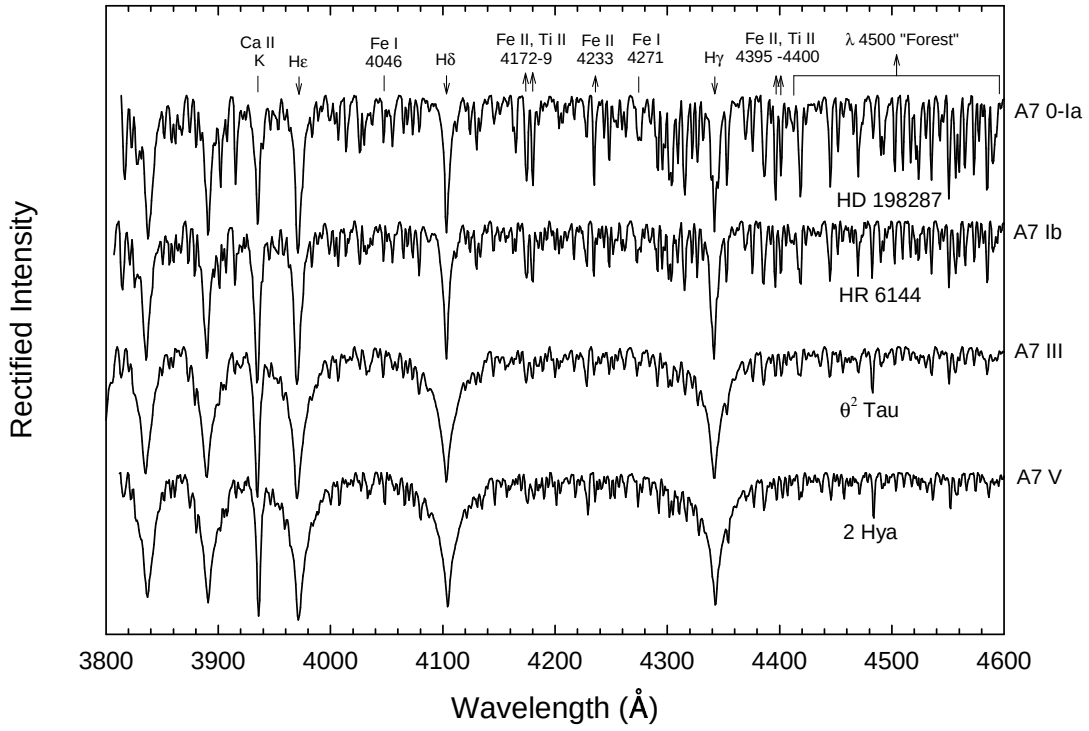

Figure 4.2 A demonstration of a luminosity sequence of A7 stars. Note how the hydrogen-line strength is not as sensitive to luminosity as to temperature, however the Fe II and Ti II lines show a noticeable increase in strength with increasing luminosity.

The spectrum of an Am star is set apart from the spectrum of a normal A-type star in that its metallic-line type appears to be of a cooler temperature than the hydrogen-line type, and the Ca II K-line type appears to be of a hotter temperature than the hydrogen-line type. In Figure 4.4 we see that the Ca II K-line of the classic Am star

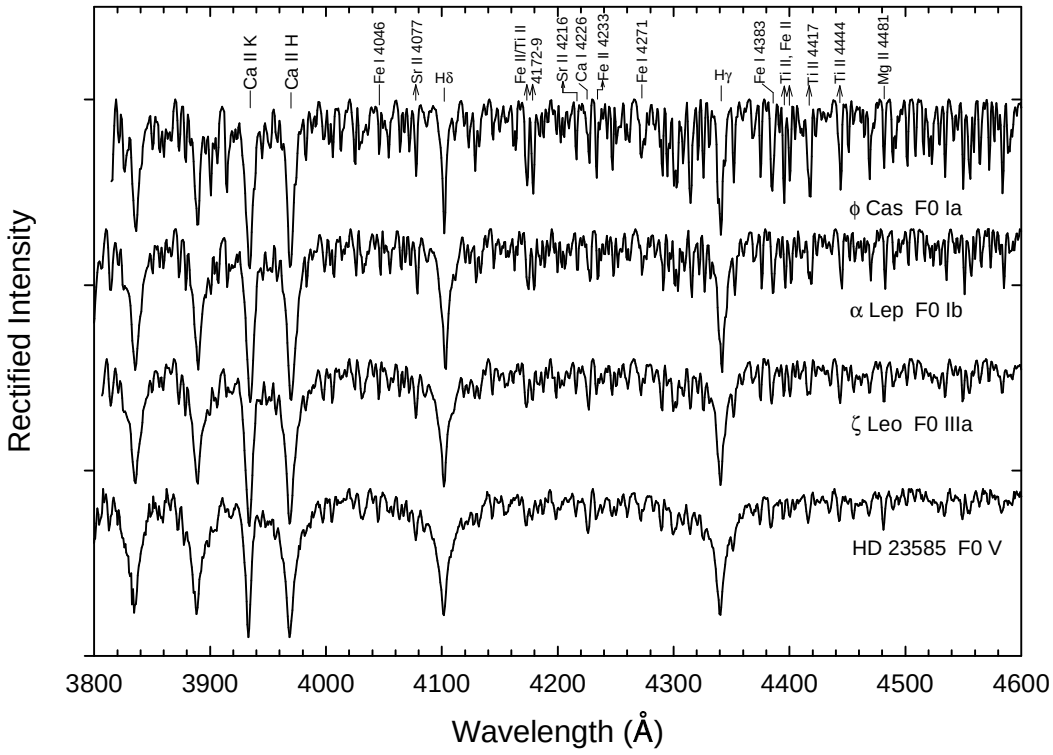

Figure 4.3 A demonstration of a luminosity sequence of F0 stars. In contrast to the luminosity sequence for A7 stars, it can be seen that the hydrogen lines exhibit almost no sensitivity to luminosity, predominantly in the giant to supergiant luminosities for F0 stars. Note the strong sensitivity of lines of Fe II and Ti II to luminosity.

63 Tau is closer to that of an A1.5 standard star, indicating a hotter temperature class than is indicated by the hydrogen lines which are a good match with the A9 standard star 30 LMi. In addition, we see that the overall metallic-line spectrum for 63 Tau is closer to that of an F3 star, cooler than the temperature type indicated by the hydrogen lines.

An A- or early F-type star is considered to be Am or Fm (respectively) star if the difference between the Ca II-K line type and the metallic-line type is at least five

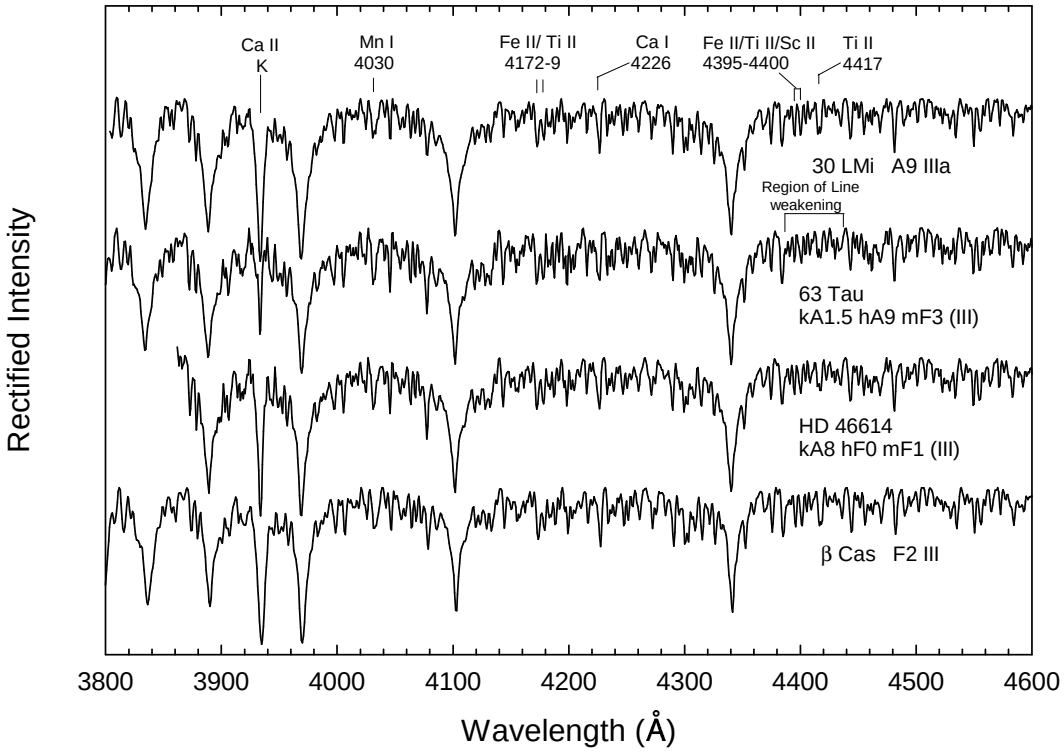

Figure 4.4 Two Am stars, 63 Tau and HD 46614, are compared with two MK standards, 30 LMi and β Cas.

subclasses. For example, a star with a Ca II-K line type of A7 and a metallic-line type of F2 would be classified as Am. A difference of less than five subclasses results in a categorization of proto-Am or proto-Fm. Am, Fm and ρ Puppis stars, because of the discrepancies between classification features, are classified for each feature separately. An example spectral type of an Am star is kA3hA7mA9 (III), denoting a Ca II K-line type of A3, a hydrogen-line type of A7, a metallic-line type of A9 and a luminosity classification of III (giant).

In addition to the hydrogen-line, metallic-line and Ca II K-line discrepancies, Am stars also exhibit a discrepancy in their luminosity classification as mentioned in the

Introduction. In Am stars exhibiting this Anomalous Luminosity Effect, the strength of the Fe II/Ti II blends in the $\lambda\lambda$4395-4480 region will often be comparable to the strength of the Fe II/Ti II blends in this same region of a dwarf star. Simultaneously, the strength of the Fe II/Ti II blend in the $\lambda\lambda$4172-4179 region will be comparable to the strength of the Fe II/Ti II blend at this same region in a giant star, but in some extreme cases it will resemble that of a supergiant. In the case of a star exhibiting the Anomalous Luminosity Effect, it is common practice to determine the luminosity classification based on the Fe II/Ti II blend at λ4172-4179 and that luminosity type should be enclosed in parentheses in the classification. Referring back to Figure 4.4, we see this Anomalous Luminosity Effect illustrated. Note in 63 Tau that the Fe II/Ti II blends in the $\lambda\lambda$4395-4480 region, in particular, are weaker than those in the same region in the giant standard stars. Also note that the Fe II/Ti II lines at $\lambda\lambda$4172-4179 are about same strength as the those in the standard stars, resulting in a luminosity classification of giant for the Am star.

It can now be seen in Figure 4.5 how the ρ Puppis stars exhibit the abundance pattern of Am stars. Notice that the Ca II K-lines of both ρ Puppis stars are weak for their hydrogen-line types. The metallic-line types tend to be the same as the hydrogen-line types, however, they are indeed "late," as the hydrogen-line type necessary for the ρ Puppis classification is typically F5. The exhibition of the Anomalous Luminosity effect however, is extreme in both ρ Puppis stars. In particular, HD 103877 has a $\lambda\lambda$4395-4480 region that is drastically weaker than that region in the giant standard star 60 UMa, while it has an Fe II/Ti II blend at $\lambda\lambda$4172-4179 that is notably stronger than this same blend in the giant standard.

Because ρ Puppis stars possess abundance patterns similar to Am stars, we identified stars as ρ Puppis if they (1) showed Am-type discrepancies in their hydrogen-line,

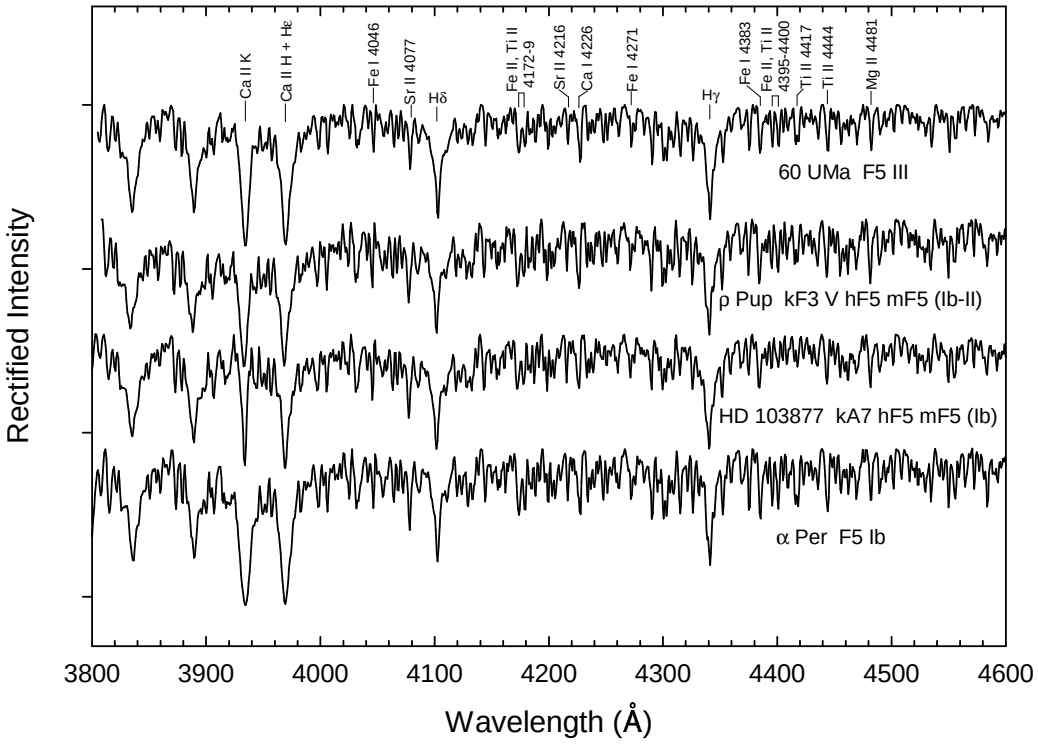

Figure 4.5 Two ρ Puppis stars, ρ Puppis itself and HD 103877, are compared with two MK standards, 60 UMa and α Per.

Ca II K-line and metallic-line types, (2) exhibited the Anomalous Luminosity Effect, and (3) had hydrogen-line types of F3 or later. A table of the spectral classifications of the ρ Puppis candidates observed at the Dark Sky Observatory is presented below in Table 4.3 for stars selected from the the Mermilliod Catalog and in Table 4.4 for stars selected from the Houk Catalog.

Table 4.3 Spectral Classifications and Notes

ρ Puppis Candidates Selected from the Mermilliod Catalog

HD	BD	Mag	Classification	Notes
1169	7.00023	7.588	kA7hF0mF0 (III)	proto Fm mild ALE
1601	48.00084	6.473	F6 II	
1607	21.00025	8.68	kA5hF5mF5 (III)	ρ Pup, strong ALE
1616	9.0003	8.62	F0 V(n) mA6	metal weak
2424	15.00062	7.685	kF0hF5mF5 (III-IV)	ρ Pup, strong ALE
5537	47.0026	8.48	kA3hA9mF0 (II+)	extreme Am, pronounced ALE
6843	51.00239	7.905	F7 V Sr	composite spectrum
8368	23.00184	8.206	kA6hF0mF0 (III)	Fm
9800	47.00463	7.459	kF2hF3mF5 (III)	early ρ Pup, mild ALE
11316	75.00076	6.965	kA7hF3mF5 (III)	early ρ Pup, enhanced Sr
13474	65.00239	6.051	G + A	composite G and A
13729	-3.0034	7.321	kA5hA9mF5 (III)	extreme Am, pronounced ALE
17431	44.0058	8.55	knA8hA8mF2 (IIIp) (EuSr)	blend of Am and late Ap peculiarities, broad but truncated K-line
17905	31.00497	6.608	F5 II-III (Sr)	may be evolved Ba dwarf
18358	9.00381	8.85	kF0hF0mF5 (III)	late Fm, note strong Eu
18752	14.00503	7.777	kF1hF5mF5 (II-III)	mild ρ Pup
18904	10.00404	8.104	F5 III+ (Sr)	slightly peculiar

Spectral Classifications and Notes (Mermilliod) 4.3 – Continued

HD	BD	Mag	Classification	Notes
19430	16.00392	8.187	kA5hF5mF5 (III+)	ρ Pup, very strong ALE
19447	16.00393	7.671	kA6hF1mF2 (IV)	Fm, strong ALE, asymmetrical K-line profile
20656	12.00467	7.123	F7	composite F7 and early F dwarf?
21439	7.00511	7.595	kF0hF2mF5 (III)	late Fm, possible mild ρ Pup based on late metallic-line type?
22128	-7.00624	7.595	kA6hF2mF2 (V) (SrBa)	Fm
22129	-7.00625	7.587	F0 III-IV	
23143	3.00517	8.44	kF1hF1mF5 (III)	late Fm, possible ρ Pup based on late metal type?
24571	18.00557	7.824	kF0hF5mF6 III CH+0.4	peculiar star, K-line narrow but deep, G-band too strong for H-line type
25518	38.00838	8.164	F5 III+	
25007	80.00125	5.105	F8 V+	composite spectrum
25499	52.00759	8.041	F1 III	
26598	10.00548	8.088	kF2hF1mF2 III (Sr)	evolved Ba dwarf?
26815	31.00733	8.057	kA5hF1mF2 (III)	extreme Fm, strong ALE
28353	45.00941	7.831	kA7hF5mF5 (II-III)	ρ Pup, strong ALE, enhanced Sr and Ba

Spectral Classifications and Notes (Mermilliod) 4.3 – Continued

HD	BD	Mag	Classification	Notes
28449	11.00618	8.325	kA5hF1mF3 V	no ALE, strong Sr and Ba
28976	22.00712	6.749	F5.5 III	
30050	-10.00993	7.771	kF1hF5mF5 (IV) (Sr)	possibly ρ Pup or Ba dwarf
31982	9.00705	7.819	F5 II+	
32444	54.00858	8.53	kF0hF5mF5 (III+)	ρ Pup, strong ALE
33054	8.00866	5.33	kA4hF1mF3 (III)	hyper Fm
33291	-17.01031	8.555	F6 II (k)	note K line emission
33268	36.01027	8.57	F6 III-IV	
34318	-11.01117	6.46	F8 V	composite spectrum
32196	85.00074	6.488	kA6hF1mF5 (III)	hyper Fm, strong ALE, moderate Sr II, deep H-lines
36422	44.01232	7.686	G5 III + A	composite spectrum, note strong CN band
37154	57.00901	8.85	kF1hF1mF5 (II)	late Fm, possible ρ Pup based on high luminosity type and late metallic-line type
37819	28.00856	8.074	F5 II	
38573	20.011	7.349	kA5hF0mF5 (III+)	hyper Fm
40958	41.01343	8.586	kF5hF0mF5 II-III	curious star, overall match to F5 II-III except H-lines

Spectral Classifications and Notes (Mermilliod) 4.3 – Continued

HD	BD	Mag	Classification	Notes
41786	21.01125	7.288	kF2hF0mF5 III	peculiar star, composite??
41724	35.01345	7.622	kA4hF1mF1 (III)	extreme Fm
42097	-19.01364	8.19	kF1hF5mF5 (II-III)	ρ Pup
42438	-9.01349	8.481	kF1hF1mF5 (III)	late Fm, strong ALE
253926	16.01055	9.621	A8 V(n) kA6	may be sl metal weak?
43478	32.01246	7.515	F2 V	composite spectrum
43623	39.01584	8.746	kA8hF0mF2 (III)	Fm, mild ALE
44734	-9.01439	9.572	F5 III-IV	rough classification but appears normal
47033	0.01504	8.82	kA9hF0mF2 (III)	proto Fm, mild ALE
47525	23.01446	7.431	F5+ III+	
47480	37.01558	8.684	kA6hF1mF5 (III)	hyper Fm, very strong Ba
47888	9.01345	6.544	F8 + G5 III	composite spectrum of F8 and G5?
49636	18.01365	8.045	F6	composite spectrum
50186	25.01482	7.41	kA3hF0mF0 (III-IV)	extreme Fm
50926	57.01019	8.23	kF1hF1mF2 III	possibly early Ba dwarf based on no ALE, almost normal K-line, and strong Sr II
51424	-7.01642	6.333	F6	composite spectrum
55997	16.01429	9.181	F1 V mA7	mild λ Boo?/blue straggler

Spectral Classifications and Notes (Mermilliod) 4.3 – Continued

HD	BD	Mag	Classification	Notes
58452	37.01718	8.78	kA7hA9mF2 (III)	Am
66094	-8.02186	7.255	F7 + F8	composite spectrum
66068	54.01195	7.043	kA4hF0mF2 (III-IV)	extreme Fm, clear ALE, strong Sr II
67230	7.01921	7.636	kF2hF1mF5 (II-III)	mild late Fm
70318	18.01923	8.23	kA7hF1mF5 (III)	hyper Fm
72792	56.01314	7.61	kA8hF2mF5 (III)	hyper Fm, probably early ρ Pup
77081	4.02098	8.96	kA5hF0mF3 (III)	hyper Fm
77601	49.01801	5.4	F6 III-IV	
80316	-19.02674	7.804	A9 IIIs	
82072	-2.02906	7.41	F8	composite spectrum
83270	69.00528	7.541	kA5hF5mF5 (III)	ρ Pup
85030	34.02038	7.901	F5.5 III+	
86167	29.01977	8.38	kA9hF0mF2 (III-)	proto Fm
86458	69.0055	8.022	kF0hF4mF4 (III)	mild ρ Pup
87093	7.02227	8.699	kA6hF5mF5 (III)	ρ Pup
	47.01812	9.56	kA5hF0mF3 (III)	hyper Fm, fairly normal Sr II but pronounced ALE and weak K-line
93992	37.02127	8.84	kA7hF1mF5 (III+)	hyper Fm
95899	4.02415	7.228	kA7hF0mF0 (III)	peculiar star, Hδ narrower than Hγ
96391	72.00515	7.08	kF0hF2mF4 (III) (SrEu)	late Fm, mild ALE

Spectral Classifications and Notes (Mermilliod) 4.3 – Continued

HD	BD	Mag	Classification	Notes
98880	45.01916	8.061	kA7hF2mF5 (III) (Sr)	hyper Fm, asymmetrical K-line, mild ALE
100654	36.02198	8.57	kA9hF5mF5 (II)	evolving ρ Pup
100707	-19.03302	7.784	F6 V	composite spectrum
101320	27.02044	8.26	A3 Vs	
102509	21.02358	4.52	F6 V (Sr II)	composite spectrum
102942	34.02264	6.237	kA9hF0mF5 (II)	late Fm
103877	18.02546	6.786	kA7hF5mF5 (II)	canonical ρ Pup
105217	21.02392	8.893	F5 II	
105281	-9.03434	8.23	kA5hF0mF5 (II)	hyper Fm, clear ALE
105702	6.02559	5.713	kF0hF0mF5 (II-III)	late Fm
106112	78.00412	5.155	kA5hF1mF4 (III)	hyper Fm, clear ALE
108464	42.02307	6.519	F6	strange composite spectrum
109782	21.02436	7.673	kF1hF1mF5 (III)	late Fm
110026	15.02491	8.084	kA4hF1mF5 (III)	hyper Fm
110026b			F8 V (Sr)	peculiar star, need new observation to clarify
111702	-11.03378	8.823	kF0hF0mF5 (II-III)	late Fm
111918	59.0147	8.19	A9 III	fairly normal, sl broad H-lines
112310	75.00489	8.384	kA5hF0mF5 (II-III)	hyper Fm
117517	-15.03682	8.197	kA8hA9mF2 (III)	Am, note strong Mg II 4481 Å

Spectral Classifications and Notes (Mermilliod) 4.3 – Continued

HD	BD	Mag	Classification	Notes
120901	-17.03949	6.961	F6	strange composite spectrum
121248	14.02678	7.85	A9 IIIp (EuSrCr)	note truncated K-line, peculiar Ap
124587	29.02508	6.82	kA5hF1mF5 (III+)	hyper Fm
125061	-13.03865	8.818	F4 II-III	
125335	11.02662	7.23	kA7hF0mF4 (III)	hyper Fm, note strong Ba II
126031	15.02702	7.62	kA4hF1mF3 (V)	hyper Fm, however, does not appear evolved
134417	62.01385	8.82	kA5hF1mF5 (III)	hyper Fm
136884	21.02764	8.21	kF2hF1mF5 (III)	mild late Fm, mild ALE, late metals
141798	-12.0435	8.731	kA8hF1mF5 (III)	hyper Fm, strong ALE
141898	-12.04353	7.479	F6 III	composite spectrum
143588	12.02933	8.101	F5 III-	
144208	37.02708	5.8	F6 III	strange composite spectrum
149748	63.01281	7.366	kA5hF1mF5 (III+)	hyper Fm
151070	23.02984	6.871	F3 IIIs	
151307	-2.04246	8.255	kF1hF1mF5 (III+)	late Fm, although unusual
151604	42.02747	7.97	kA5hF1mF5 (III-IV)	hyper Fm, extreme ALE
151878a	36.02783	7.223	kA5hF1mF5 (III-IV)	hyper Fm

Spectral Classifications and Notes (Mermilliod) 4.3 – Continued

HD	BD	Mag	Classification	Notes
151878b			F2 V	
153450	46.02243	8.6	A7 Vp (SrEu)	peculiar star, note extremely strong Sr II
163467	52.0211	8.511	kA6hF1mF2 (III)	Fm, note strong ALE and Sr II
166067	46.02426	7.457	kA8hF1mF5 (III)	hyper Fm
167944	12.03446	7.223	F6	composite spectrum
174344	49.02871	7.195	kF1hF2mF2 (III)	proto Fm, but strong Sr II at 4077 Å, pronounced ALE and strong Ba II and Eu II
174984	25.0365	7.156	kF2hF5mF5 (III)	ρ Pup, possibly evolved based on smaller K-line discrepancy
176391	42.03206	8.33	F5 III+	
176942	10.03762	7.292	kA5hF1mF5 (III)	hyper Fm, pronounced ALE
179143	37.03357	6.814	kA6hF1mF5 (II-III)	hyper Fm
179491	5.04069	7.46	F6	composite spectrum
183303	8.04112	7.457	kF1hF2mF5 IV	late Fm
186155	45.02949	5.07	F5 II-III	MK std HR 7495
188854	46.02807	7.617	kA5hF1mF5 (III)	hyper Fm
190887	12.04226	7.291	F5 (II-IIIp) (SrEu)	ρ Pup, probably evolved, normal Eu suggests not Ba dwarf

Spectral Classifications and Notes (Mermilliod) 4.3 – Continued

HD	BD	Mag	Classification	Notes
192342	23.03935	6.598	kA2hF0mF5 (III)	hyper Fm
193389	15.04128	7.568	F5.5 II-III	
198031	-19.05928	6.811	F5 III+	
198743	-9.05598	4.729	kA5hF1mF3 (III)	hyper Fm
198896a	43.03746	7.94	G9 III	
199043	24.04266	8.6	kA7hF4mF5 (III)	ρ Pup
201032	62.01889	7.346	kA7hF5mF5 (III)	ρ Pup
203522	2.04348	6.544	F6 V	composite spectrum, note: SB
204751	66.01404	7.93	kA6hF1mF5 (III)	hyper Fm
208713	62.02004	7.229	F6	composite spectrum
211856	11.04779	7.626	F2 + F3 V	SB2, possibly first detection?
212391	65.01759	6.619	A + G	composite spectrum
212671	12.0482	8.85	kA5hF1mF5 (II-III)	hyper Fm
213233	50.03733	7.873	F7 II	
213235	3.04713	5.502	kF0hF2mF5 (III-IV)	late Fm (DAO spectrum shows shell star characteristics)
216774	17.04833	7.674	kA7hF1mF5 (III-)	hyper Fm
216879	22.04742	7.378	kF1hF1mF3 (III)	mild late Fm, mild ALE
217602	15.04748	8.256	kA2hF0mF5 (III)	hyper Fm, strong ALE
218634	7.04981	5.124	M2 V	
218925	49.04065	6.808	kA9hF5mF5 II-III	ρ Pup, but ALE very weak

Spectral Classifications and Notes (Mermilliod) 4.3 – Continued

HD	BD	Mag	Classification	Notes
219675	17.04891	6.727	kF0hF2mF5 (II-III)	late Fm
219735	42.04627	8.066	F0 IIIa	
221072	62.02234	8.285	F4 V	SB2
221890	-9.0622	7.186	F6 III+	
222146	-2.06	7.697	kF0hF1mF5 (II-III) (SrEu)	late Fm, strong ALE
222355	42.04726	7.548	F6 IV	probable composite spectrum, ambiguous results from other works
223839	11.05068	7.277	kF2hF0mF5 (III+)	possible composite or unusual Fm
224405	47.04335	8.49	kA9hF1mF2 (III)	proto Fm

Table 4.4 Spectral Classifications and Notes

Houk Catalog

HD	BD	Mag	Classification	Notes
728			K0 IV	
3024			kA7hA9mF2 (III)	Am, mild ALE, strong Sr II
3649			F4 V	
4630			kA7hA9mF0 (III)	proto Am, mild ALE
7119			kA6hA9mF0 (III)	Am, strong Sr II, pronounced ALE
7133			kF1hF3mF5 (III)	ρ Pup, very strong Sr II, strong ALE, enhanced Eu and Ba
8251			kA8hF0mF0 III+ (Sr)	proto Fm, strong Sr II, weak ALE
15306			F4 V mF2 Sr	canonical Ba dwarf, slightly metal weak
16641			kA6hA7mF0 (III)	Am, mild ALE
16932			kA5hF0mF0 (III-IV) (Sr)	Fm
18460		8.44	kA7hA8mF5 (III)	extreme Am, mild ALE
19108	-9.00583	8.29	kF1hF0mF2 (IV)	proto Fm, possibly evolved?
20431			kA7hA9mF2 (II-III)	Am, strong Sr II
21769			kA4hA5mA6 (V)	proto Am
24925			kA7hF0mF0 (III)	proto Fm
25305			kA2hA7mA7 (V)	Am, mild ALE

Spectral Classifications and Notes (Houk) 4.4 – Continued

HD	BD	Mag	Classification	Notes
25515			kA8hF1mF2 (III)	Fm enhanced Sr and Ba
29870	-1.00702	6.731	kF2hF5mF5 (III-)	ρ Pup
30331			kA4hF0mF2 IIIp (SrBa)	peculiar star, H*gamma*:F0 but H*delta*:F2?, K-line is weak, huge Sr and Ba!
33692			kA7hF1mF2 (III)	Fm
33959			A9 V	
38548			A7 Vp kA6 (SrEu)	curious Ap star
39390			kA6hF1mF1 IV Sr	possible early Ba dwarf
41770			kF2hF5mF5 (III)	ρ Pup, strong Eu
46378			F5 III	violet appears veiled
46614			kA8hF0mF1 (III)	proto Fm
47606			A8 II-III	enhanced Sr
51673			kF1hF1mF2 (III)	proto Fm
52010			kF2hF5mF5 (II-III)	ρ Pup, clear ALE, strong Sr II, massive Ba and strong Eu
54277			kA9hF5mF5 (III)	ρ Pup
58340			kA8hA8mF0 (III)	proto Am
68333			kA5hA8mF0 (IV)	Am
68957			kF0hF1mF5 (III-IV)	late Fm
69682			kA8hF1mF2 (III-IV)	Fm
73670			F0 III	

Spectral Classifications and Notes (Houk) 4.4 – Continued

HD	BD	Mag	Classification	Notes
81772			kA8hA9mF0 III	proto Am, strong Sr, weak ALE, enhanced Ba, only sl enhanced Eu
86029			kA4hF0mF2 (III)	extreme Fm
92054			kA7hA8mF0 (III-IV) (Sr)	proto Am
92751	-5.03125	9.145	kF0hF1mF5 (III) (Eu)	late Fm
100565	-4.03096	6.771	kA7hF1mF3 (III)	late Fm, strong Eu
103550			kA7hA7mF0 (II)	proto Am, clear ALE
109957			F0 III kA9	peculiar star, weak K-line
122370	-9.03832	8.654	F5 III-	
176716			kA5hA9.5mF0 III	peculiar star, need new spectrum to clarify
182835			F5 Ib-IIp	fairly normal, but note weak Ca I 4226 Å
192665			kA7hF4mF5 (III)	ρ Pup, strong ALE
197721			kA8hA9mF0 (III)	proto Am
197778			kA7hF1mF5 (III)	hyper Fm, clear ALE, strong Eu, only sl strong Sr II
205813			F0 IV+	
213143	20.05166	7.77	kF0hF1mF5 (III)	late Fm

Spectral Classifications and Notes (Houk) 4.4 – Continued

HD	BD	Mag	Classification	Notes
213634			kA7hA7mA7 II	peculiar luminosity discrepancies: H-lines A7 V-III, metallic-lines A7 II)
219068			kA8hF0mF0 (II)	proto Fm, pronounced Am characteristics despite marginal k/h/m discrepancies
221446			kF1hF1mF4 (III)	mild late Fm, pronounced ALE
225184			kA5hF1mF1 (III-IV)	Fm, clear ALE
221789		8.2	kA7hA9mF2 IV	Am, though no detectable ALE

I found in the classification process that most of the candidate stars were either Am, Fm, ρ Puppis, Ba dwarf or a binary system exhibiting a composite spectrum, usually consisting of an F-type and a G-type star. I further divided the Fm classification using the term "extreme" to denote Ca II K- and metallic-line discrepancies larger than six spectral subclasses, the term "late" to denote metallic line types of F3 or later, and the term "hyper" to denote Fm stars that were both "extreme" and "late." Because the classification of ρ Puppis is reliant on a late hydrogen-line type, and in some cases, an extremely late metallic-line type, I distinguished the following groups: Am, Fm, Late/Hyper Fm, ρ Pup, Ba dwarf and Composite. It can be seen in Figure 4.6 that the number of late Fm-type stars is double that of the Fm-type stars, as well as the ρ Puppis stars. This trend might lead one to think that there is no natural progression from Fm to ρ Puppis, suggesting that we are seeing stars that are subject to mass-transfer from an AGB companion star.

In addition, it can be seen in Figure 4.7 that there is a bimodal distribution of all of the ρ Puppis candidate stars according to hydrogen-line type, the predominant determining factor of whether or not an Fm star should be considered to be ρ Puppis. There is a peak in the number of stars at a hydrogen-line type F1, after which the number of stars for each type drops off drastically until we see another sudden peak at F5. This implies that Fm stars typically disappear around F2 in accordance with Smith (1973), but then there is a sharp peak of ρ Puppis stars, at later (cooler) types. The fact that both the Mermilliod catalog stars and the Houk catalog stars show this same trend implies that this is likely a real trend. It also suggests that the ρ Puppis group may be disjunct from the Am/Fm stars. Both trends shown in Figure 4.6 and in Figure 4.7 are motivations to explore the mass-transfer (Ba dwarf) hypothesis. However, the bimodal distribution of Fm stars according to hydrogen-line type shown

in Figure 4.7 may result from the evolutionary process itself. While this will be considered in the Discussion and Conclusions section, much further investigation is required on this point.

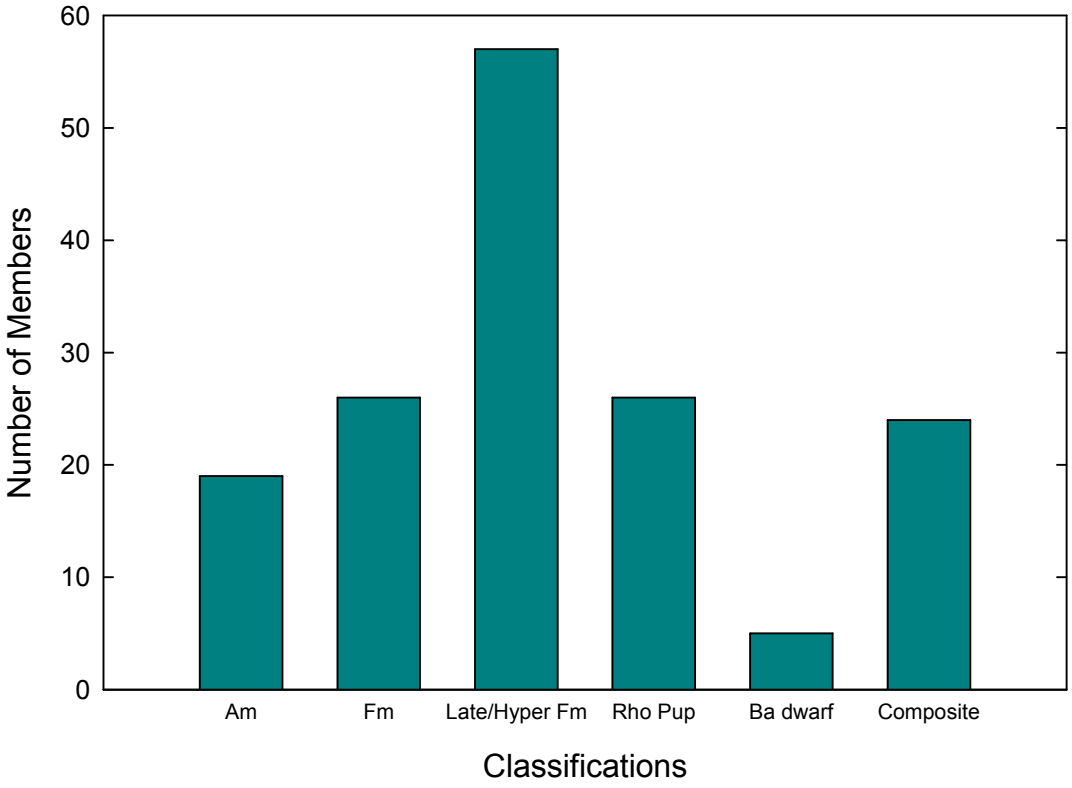

Figure 4.6 A histogram of the spectral classification types of all the ρ Puppis Candidates.

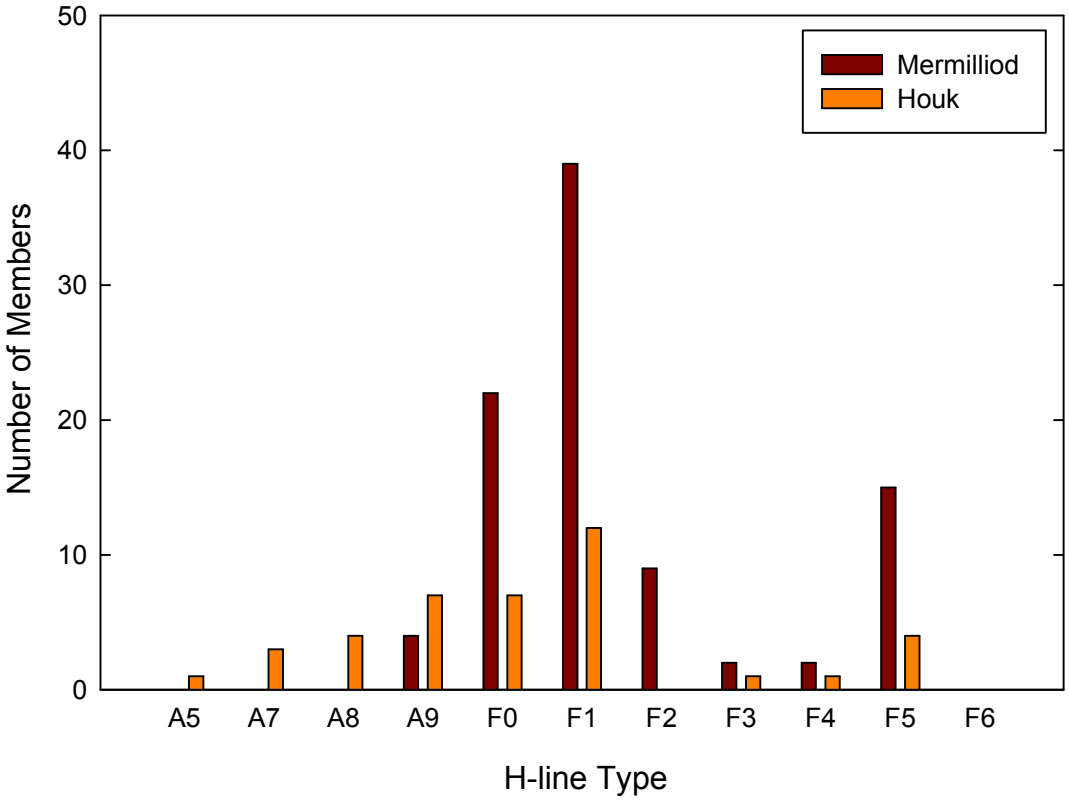

Figure 4.7 A Histogram of the H-line types of all the ρ Puppis Candidates.

Chapter 5

Abundance Analysis

An abundance analysis was carried out for seven of the ρ Puppis candidates observed at DAO, as well as three additional ρ Puppis candidates for which I obtained high-resolution ($R = 42000$) spectra from the ELODIE archive maintained at the Observatoire de Haute-Provence (OHP) (Moultaka *et al.* 2004).

I calculated initial values for the stellar parameters, including effective temperature ($T_{\rm eff}$), surface gravity ($\log(g)$), microturbulent velocity ($\xi_{\rm t}$), metallicity ($[M/H]$) and rotation ($v\sin i$) using an X Window System program, xfit34, written by Richard Gray (Gray *et al.* 2003). The program xfit34 allows the user to compare the observed DSO spectrum and fluxes from Strömgren uvby and other photometric systems with synthetic spectra and fluxes computed with the basic physical parameters entered by the user. The program calculates a χ^2 difference between the observed and synthetic spectra and the observed and synthetic fluxes. The synthetic spectra and fluxes used by xfit34 are calculated with the stellar spectral synthesis program SPECTRUM[1] (Gray & Corbally 1994). The user then has the freedom to adjust the five parameters

[1]http://www.phys.appstate.edu/spectrum/spectrum.html.

by hand to achieve a closer fit between the synthetic and observed spectra. Once a relatively close fit is achieved, the user can apply the "Converge" optimizing facility to let the program iteratively find the best values for each parameter so that the synthetic spectrum and fluxes match the observed ones as closely as possible. See Figure 5.1.

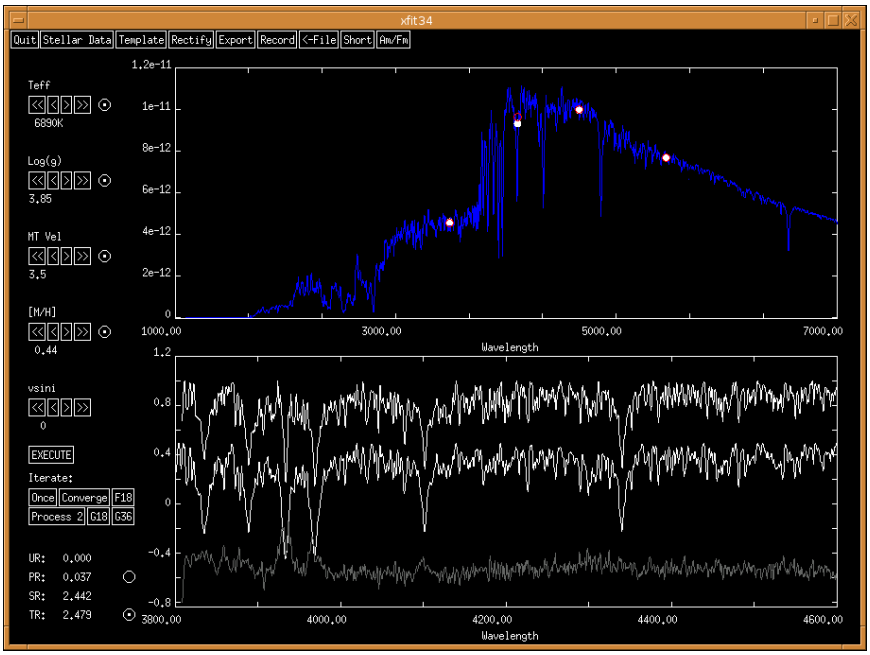

Figure 5.1 The program xfit34 loaded with HD103877.

The Am/Fm facility had to be added to the program for the purposes of calculating the χ^2 difference between the observed and synthetic spectra and fluxes, because currently, the program does not do a good job of synthesizing the weakened Ca II K-line of Am/Fm stars. The Am/Fm facility simply causes the program to ignore the portion of the χ^2 difference calculated at wavelengths that are associated with the Ca II K-line. See Table 5.1 for a list of the stellar parameters computed by xfit34 for each of the selected stars for this abundance analysis.

The xfit34 values for the stellar parameters $T_{\rm eff}$, $\log(g)$, $\xi_{\rm t}$ and $[M/H]$ were then used with Kurucz's ATLAS9 (Kurucz, 1993) program to generate initial atmospheric

Table 5.1 A list of the stellar parameters calculated by xfit34 for selected stars. The associated errors for each parameter are as follows: $T_{\rm eff}$: +/- 70 K, $log(g)$: +/- 0.1 dex, $\xi_{\rm t}$: +/- 0.5 km/s, $[M/H]$: +/- 0.1 dex.

Star	$T_{\rm eff}$	$log(g)$	$\xi_{\rm t}$	$[M/H]$
HD 13729	7150	3.75	2.7	0.56
HD 38573	7150	4.00	2.6	0.62
HD 41770	6916	3.45	4.0	0.25
HD 83270	6821	3.65	3.1	0.24
HD 102942	7364	4.00	3.7	0.59
HD 103877	6890	3.85	2.5	0.44
HD 105702	7160	4.05	3.0	0.68
HD 179143	6963	3.68	3.1	0.40
HD 179491	6387	2.77	1.1	0.27
HD 222355	6446	3.02	2.1	0.25

models for these stars. Since the ATLAS9 program can generate stellar atmosphere models only for $\xi_t = 0, 1, 2$ and 4 km/s, the initial ATLAS9 models were used as starting points in the ATLAS12 program (Sbordone *et al.* 2004; Sbordone 2005), which can generate models for any value of the microturbulent velocity.

Another X Window System program called xeqw3, written by Richard Gray, was used to measure the equivalent widths of certain spectral lines of interest. This program requires the user to load an observed spectrum of a star. It then places an adjustable synthetic spectral line on top of the observed spectrum for comparison. See Figure 5.2.

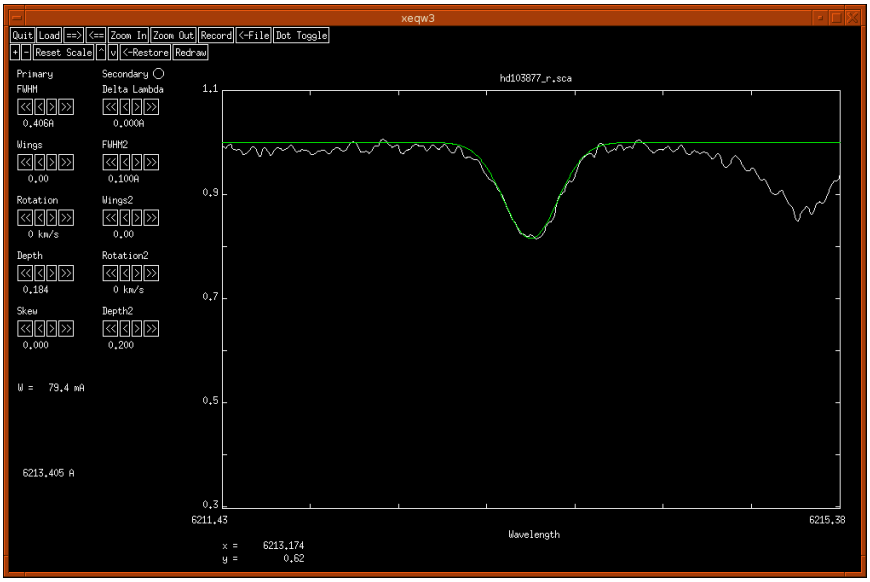

Figure 5.2 The program xeqw3 using 1 synthetic spectral line to match the observed line.

The synthetic spectral line has a pseudo-Voigt profile, calculated by convolving a Gaussian profile with a Lorentzian profile. This green, primary synthetic spectral line can be moved left or right in order to line it up with any particular spectral line in the observed spectrum. The profile can further be modified by adjusting the five parameters FWHM (Full Width at Half Maximum), wings, rotation, depth and skew

until the user has achieved the closest possible fit of the synthetic line to the observed one. The program reports a new calculation of the equivalent width of the synthetic line for every adjustment of the parameters. In the case where the spectral line to be measured is in close proximity to a neighboring spectral line, the user can apply a blue, secondary synthetic line to account for the resulting blend. The red line is the resulting spectral feature due to both the primary and secondary synthetic lines. See Figure 5.3.

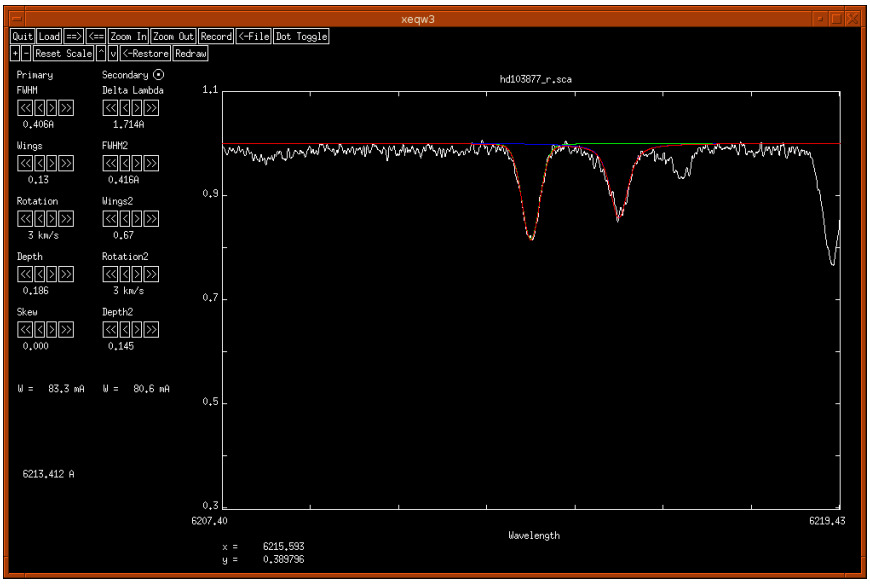

Figure 5.3 The program xeqw3 using 2 synthetic spectral lines to create a blend.

The secondary line can be adjusted to the right or left by the Delta Lambda facility which controls and reports how far the neighboring line is from the primary line. The secondary line can also be adjusted with the FWHM, wings, rotation and depth parameters in a similar fashion to the primary line.

I performed a radial-velocity adjustment of the wavelength calibration of the spectra obtained at DAO to the rest-frame of the corresponding star before using xeqw3 to measure the equivalent widths of eight spectral lines associated with Fe I in the

6100-6250 Å region. In some spectra, there were nine or ten lines that were measurable. Using the equivalent widths of the Fe I lines for each star and the appropriate ATLAS12 stellar atmosphere model, I employed an auxiliary program, BLACKWEL, which is part of the SPECTRUM spectral synthesis suite of software (Gray & Corbally 1994). BLACKWEL computes the resulting abundances for each measured spectral line for a range of microturbulent velocities. Each spectral line is therefore represented as a curve in a "Blackwell diagram." The resulting Blackwell diagram for the known ρ Puppis star, HD 103877, is shown in Figure 5.4.

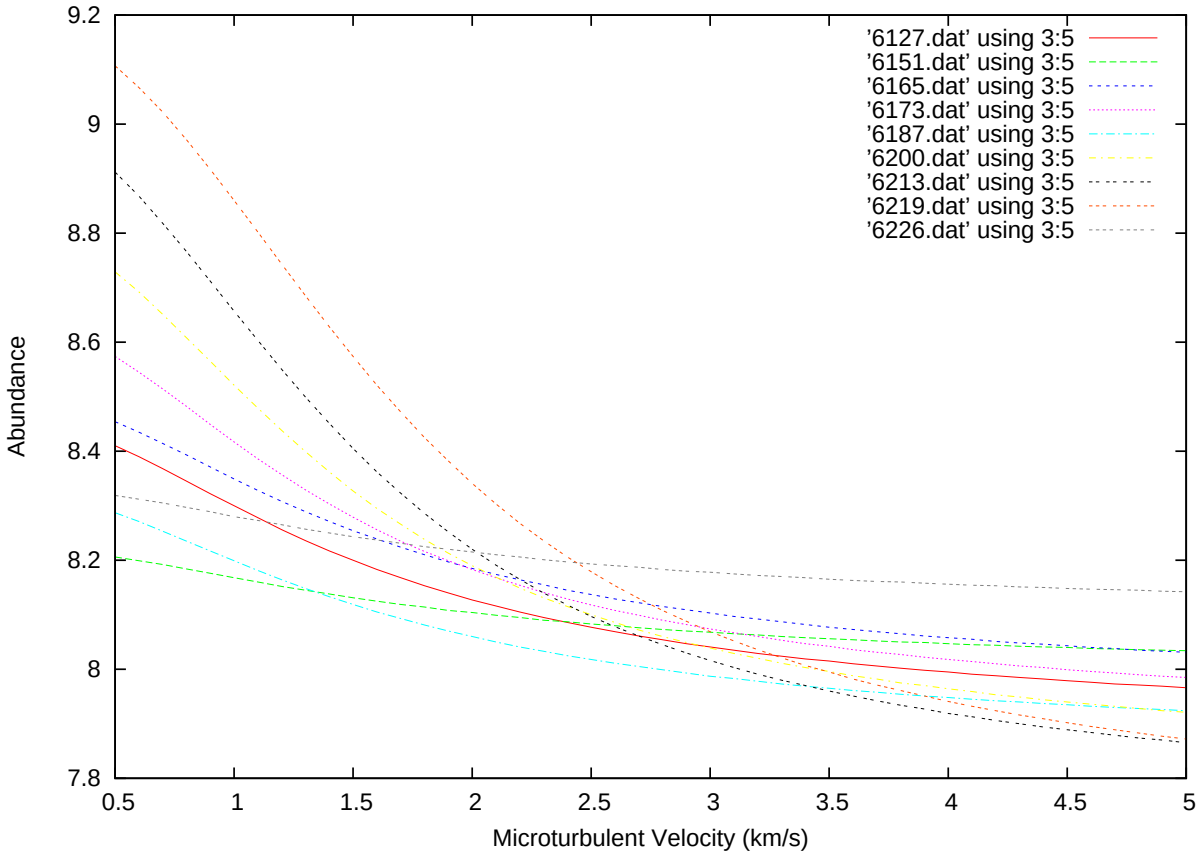

Figure 5.4 The Blackwell diagram generated from the auxiliary program BLACKWEL in the SPECTRUM suite of software. The abundance of Fe is reported here with respect to the total number of particles in the star's atmosphere.

The microturbulent velocity and the abundance for the element in question (in this case Fe I) can be determined from the Blackwell diagram in the region of "least confusion" or where the lines best converge. In the case of HD 103877, the lines converge around 2.8 km/s microturbulent velocity and yield an Fe abundance of 8.10 +/- 0.10. Note that the abundance reported by BLACKWEL is not in the form customarily reported in the literature. It is a report of $\log(A/N_{\rm total})$, or the logarithmic abundance of the element in question with respect the total number of particles in the star's atmosphere. This may easily be converted into an abundance value relative to the sun (Gray 2009). All calculated abundances in this thesis will be reported in the standard form $[X/H]$, the logarithmic abundance of the element in question relative to the solar abundance of that element with respect to hydrogen. That is

$$[X/H] = (X/H)_{\rm star} - (X/H)_{\rm sun}$$

Once the microturbulent velocity has been determined for one element from the Blackwell diagram, that value can be used in the abundance determinations of all other elements.

Another program in the SPECTRUM suite, ABUNDANCE, calculates the abundance of an element based on the ATLAS12 stellar atmosphere model, the equivalent width of a spectral line associated with that element and the microturbulent velocity derived from BLACKWEL. I measured the equivalent widths of four lines of Ca I and six lines of Si I for each star. Using those measurements, I employed ABUNDANCE to calculate abundances for both Ca I and Si I as well as to calculate the abundance values for the individual lines of Fe I. Those individual abundances are reported in Table 5.2. The final abundances for Fe I, Ca I and Si I were determined by averaging the abundances derived from each line and are listed in Table 5.3.

Table 5.2 ABUNDANCE Values for [Fe/H], [Ca/H] and [Si/H].

wavelength	HD 13729	HD 38573	HD 41770	HD 83270	HD 102942	HD 103877	HD105702	HD 179143	HD 179491	HD 222355
Fe										
6127.90	0.331	0.530		0.185	0.367	0.412	0.540	0.299	0.264	0.086
6151.62	0.523	0.560	0.155		0.547	0.317	0.567	0.324	0.349	0.396
6165.36	0.344	0.447	0.310	0.118	0.453	0.426	0.602	0.442	0.309	0.212
6173.34	0.449	0.495	0.263	0.186	0.524	0.518	0.573	0.438	0.136	0.353
6187.99	0.363	0.491	0.152	0.216	0.455	0.347	0.487	0.372	0.142	0.190
6200.31	0.428	0.613	0.173	0.188	0.364	0.398	0.538	0.247	0.257	0.270
6213.43	0.446	0.361	0.208	0.240	0.465	0.355	0.516	0.352	0.132	0.181
6219.28	0.482	0.554	0.146	0.209	0.543	0.524	0.569	0.282	0.374	-0.042
6159.36		0.606			0.527	0.461			0.362	
6226.73	0.494	0.499	0.247	0.230		0.499	0.677	0.256	0.337	0.252
6240.64			0.147		0.396					
Ca										
6161.3	-0.35	-0.35	-0.07	-0.57	-0.02	-0.5	0.39	-0.33	0.161	0.319
6163.74	-0.29	-0.39	-0.13	-0.54	-0.05	-0.54	0.27	-0.37	0.166	-0.101
6166.44	-0.29	-0.44	-0.07	-0.63	-0.08	-0.46	0.26	-0.44	0.219	0.039
6169.04	-0.45	-0.47	-0.09	-0.84	0.03	-0.45	0.46	-0.43	0.174	0.017
Si										
6125.01	0.553	0.502	0.08	0.17	0.41	0.383	0.567	0.350	0.062	-0.044
6131.56	0.234	0.349	0.18	-0.09	0.42	0.498	0.003	0.142	0.080	0.104
6131.85	0.550	0.510	0.11	0.2	0.43	0.219	0.513	0.403	0.100	0.031
6142.48	0.341	0.431	0.04	0.22	0.46	0.190	0.480	0.348	-0.013	0.042
6145.01	0.418	0.529	0.02	0.11	0.37	0.218	0.605	0.352	-0.017	0.006
6195.44	0.598	0.475	0.08	0.15		0.357	0.623	0.499	0.034	0.113
6237.31			0.04	-0.03	0.3					
6243.81			0.1	0.02	0.26					
6244.46			0.02	-0.04	0.43					

The abundances for Sr, Ba, and Eu cannot be determined with the equivalent-width method because the lines for those elements are either strongly blended with other neighboring lines, or they are composed of multiple isotopic and hyperfine components. To calculate those abundances, I used the full power of the stellar spectral synthesis program SPECTRUM to compute synthetic spectra in the regions of each of those lines. The Spectral Analysis Graphical User Interface (GUI), written by Richard Gray, was used for this purpose.

That GUI requires the input of an observed spectrum, a stellar atmosphere model, an atomic-data file, an isotope data file and a line-list file. The user is also required to set computation parameters such as wavelength range and spacing, microturbulent velocity (as calculated from the Blackwell Diagram), macroturbulent velocity, rotation, spectral resolution, spacing and shape. The user can also specify abundance ranges for up to four elements of interest. The program generates the synthetic spectra corresponding to the user-defined abundance range(s) which are then plotted on top of the observed spectrum. See Figure 5.5 and Figure 5.6.

The resolution entered into the GUI is a characteristic of the spectrograph used to obtain the spectrum loaded into the program. In the case of the coudé spectrograph at DAO, the best value for the resolution is 0.06 Å. The microturbulent velocity entered was derived from the BLACKWEL diagram, as stated previously. Then, by entering each spectrum observed at DAO in the 4415-4558 Å region into the program, I was able to first make improvements to the rotational velocity value and the macroturbulent velocity value for each star by adjusting those values until the synthesized spectrum for the entire wavelength range was more accurately fit to the observed spectrum. I then used the program in this same region to determine the Ba abundance for each star using the Ba II line at 4554 Å. I used the DAO spectra

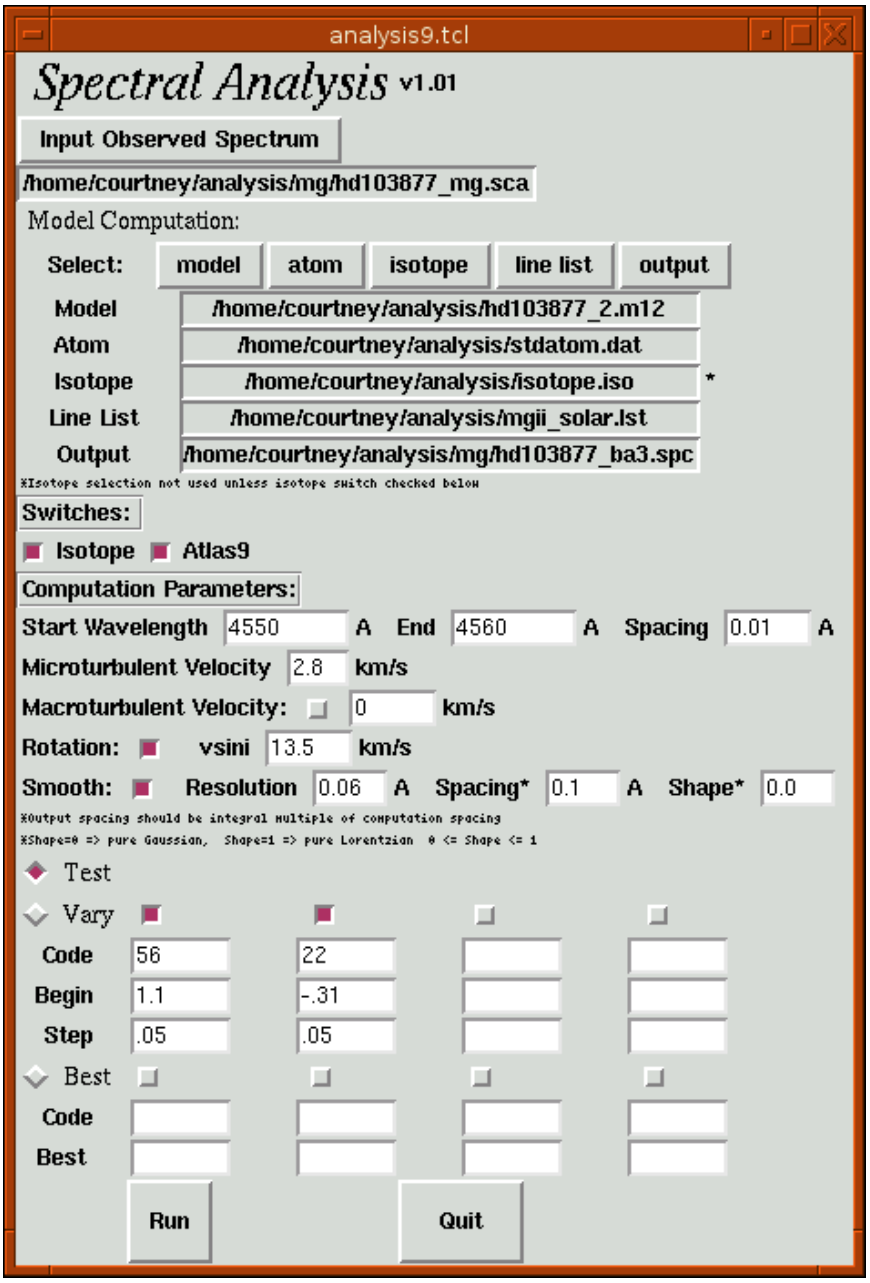

Figure 5.5 The interactive gui to control the Analysis9 suite of the SPECTRUM software.

spanning the 4077-4215 Å region to determine the Sr II abundances from the Sr II lines at 4077 Å and 4215 Å, and to determine the Eu II abundances from the Eu II lines at 4129 Å and 4205 Å. I report the resulting abundances in [X/H] form in Table 5.3.

Table 5.3 Averaged abundance values for selected stars.

Star	[Fe/H]	[Sr/H]	[Eu/H]	[Ba/H]	[Ca/H]	[Si/H]	[Ti/H]
HD 13729	0.43 +/- 0.07	1.07 +/- 0.07			-0.35 +/- 0.08	0.50 +/- 0.14	
HD 38573	0.52 +/- 0.08	1.20 +/- 0.20	1.02 +/- 0.17	1.62 +/- 0.05	-0.42 +/- 0.05	0.47 +/- 0.07	0.17 +/- 0.37
HD 41770	0.20 +/- 0.06	0.82 +/- 0.24	0.79 +/- 0.11	1.05 +/- 0.05	-0.09 +/- 0.03	0.07 +/- 0.05	0.04 +/- 0.29
HD 83270	0.20 +/- 0.04	0.73 +/- 0.13	0.82 +/- 0.85	1.22 +/- 0.05	-0.64 +/- 0.14	0.08 +/- 0.12	-0.40 +/- 0.22
HD 102942	0.46 +/- 0.07	1.38 +/- 0.16	0.98 +/- 0.10	1.57 +/- 0.05	-0.03 +/- 0.05	0.38 +/- 0.07	0.29 +/- 0.46
HD 103877	0.43 +/- 0.07	1.07 +/- 0.01	1.13 +/- 0.04	1.54 +/- 0.05	-0.49 +/- 0.04	0.31 +/- 0.12	0.13 +/- 0.15
HD 105702	0.56 +/- 0.06	1.02 +/- 0.11	0.99 +/- 0.10	1.60 +/- 0.05	0.35 +/- 0.10	0.47 +/- 0.23	0.73 +/- 0.23
HD 179143	0.34 +/- 0.07	1.15 +/- 0.18	1.23 +/- 0.10	1.72 +/- 0.05	-0.39 +/- 0.05	0.35 +/- 0.12	0.16 +/- 0.36
HD 179491	0.27 +/- 0.10	-1.93 +/- 0.42	-0.22 +/- 0.11	-0.43 +/- 0.05	0.18 +/- 0.03	0.04 +/- 0.05	0.59 +/- 0.59
HD 222355	0.21 +/- 0.13	0.39 +/- 0.07			0.07 +/- 0.18	0.04 +/- 0.06	

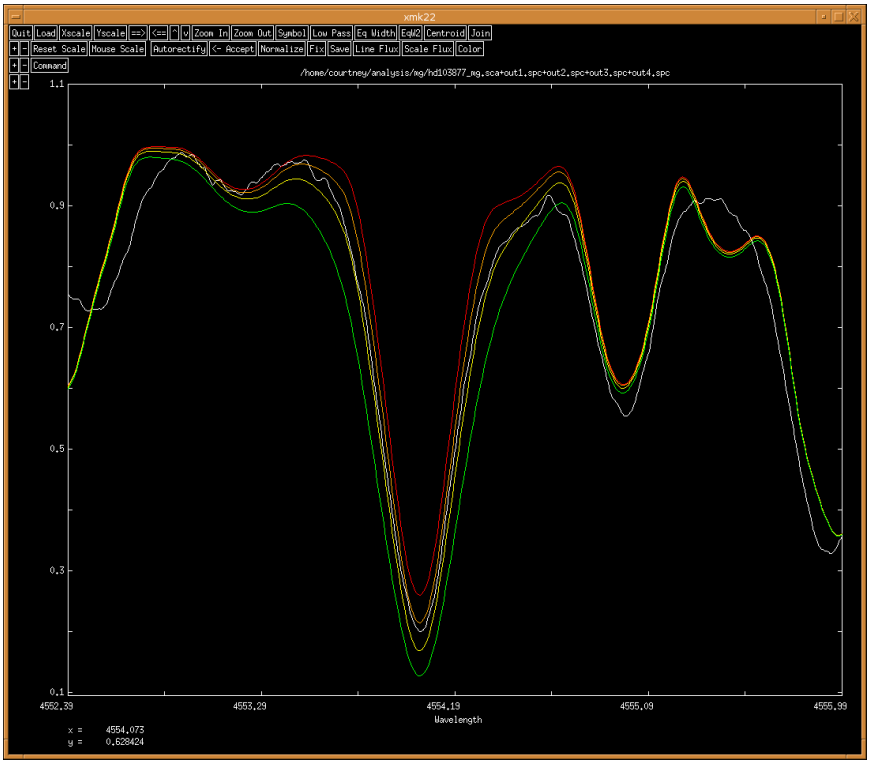

Figure 5.6 The resulting synthesized spectra computed with Analysis9 compared with the observed spectrum for HD 103877, showing a range of abundances of Ba. The object is to fit the Ba II line at λ4554.

I would like to note here that HD 179491, in terms of abundance values, is in almost all cases an outlier as shown in Table 5.3. The reason for this is that I originally misclassified the star and therefore went on to obtain high-resolution spectra of this star at DAO. Upon reclassification, this star appears to exhibit a composite spectrum of companions that have close spectral types i.e. F0 and F6. The result is a star that appears to have a weak Ca II K-line, a hydrogen-line type of F6, and a metallic-line type that appears to be around F5. I include the results here, as there were a number of composite spectra in my candidate list.

Figure 5.7 shows that barring HD 179491, there appears to exist a common abundance pattern between the Fm stars and the ρ Puppis stars. The consistent enhance-

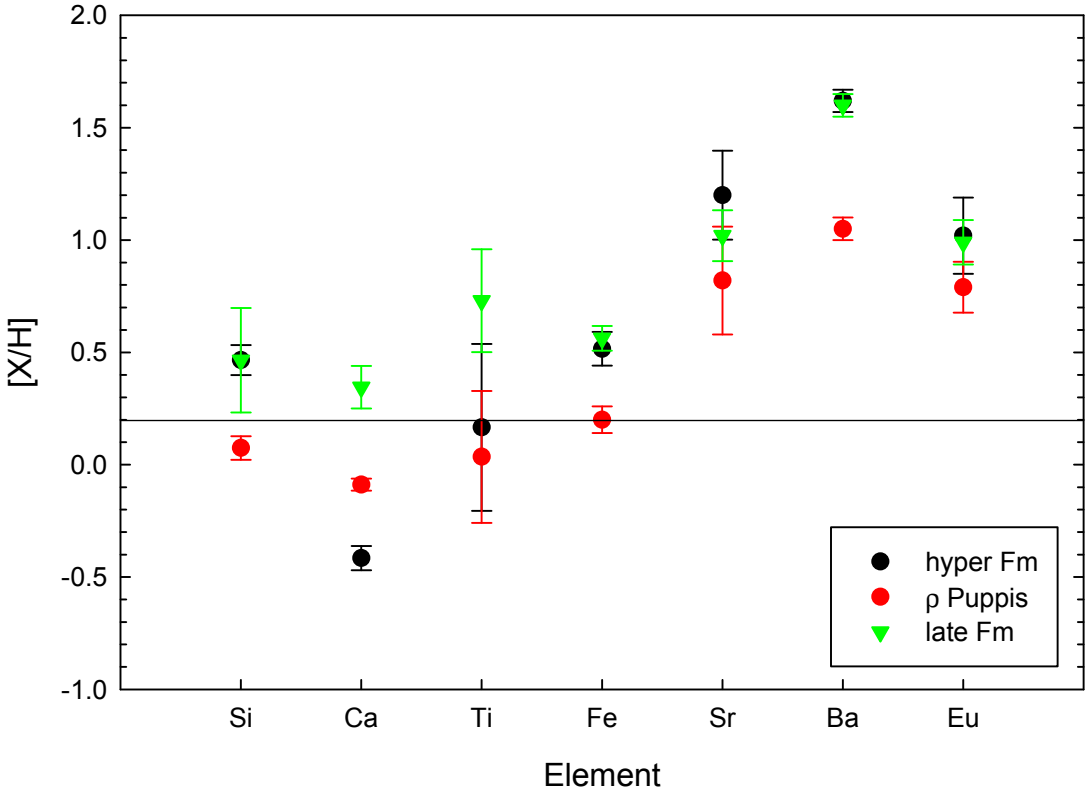

Figure 5.7 A graph of plotted abundance values for a hyper Fm star, HD 38573, a ρ Puppis star, HD 41770, and a late Fm star, HD 105702. The horizontal line indicates the elemental abundances in the sun.

ments of Fe, Sr, Ba and Eu are all similar. It has been shown that Am stars tend to exhibit near solar abundances of Ti, which is consistent with the results in Figure 5.7, however, it is presumable that the variations in the abundances derived for Ti in this study, are due to the fact that the Ti lines measured, exist in the 4415-4558 Å region where the Anomalous Luminosity Effect affects the strength of the Fe and Ti lines and blends. It is therefore not surprising that the deviations for the Ti abundances are larger than those of Sr, Ba and Eu.

Chapter 6

Discussion & Conclusions

The chemical abundance pattern of the ρ Puppis stars shows many similarities to the abundance pattern associated with Am stars. Namely, they both show enhancements of Fe, Sr, large enhancements of Ba, slight enhancements of Si, underabundances of Ca, and near solar abundances of Ti. In particular, the ρ Puppis stars show consistent and large enhancements of Eu. Because Eu is largely an r-process element, it is not produced in AGB stars, as only the s-process is active in those stars. This implies that it is unlikely that ρ Puppis stars derived their abundance peculiarities via mass transfer from a former AGB companion (now turned white dwarf) and that it is more likely that ρ Puppis stars are in a short-lived stage of evolution between the re-establishment of convection and the erasure of their peculiar abundance patterns.

In the Classifications section, I pointed out a possible contradiction to the hypothesis that the ρ Puppis stars are evolved Am stars in that we do not see a smooth transition in the number of Am-type stars through to cooler temperature types. What is seen is a sharp drop in the number of Am-type stars after F1, to a minimum at F3, and then a sharp peak at F5. No ρ Puppis star is known with an F6 or later

hydrogen-line type. However, this trend may not be inconsistent with the evolved Am star hypothesis.

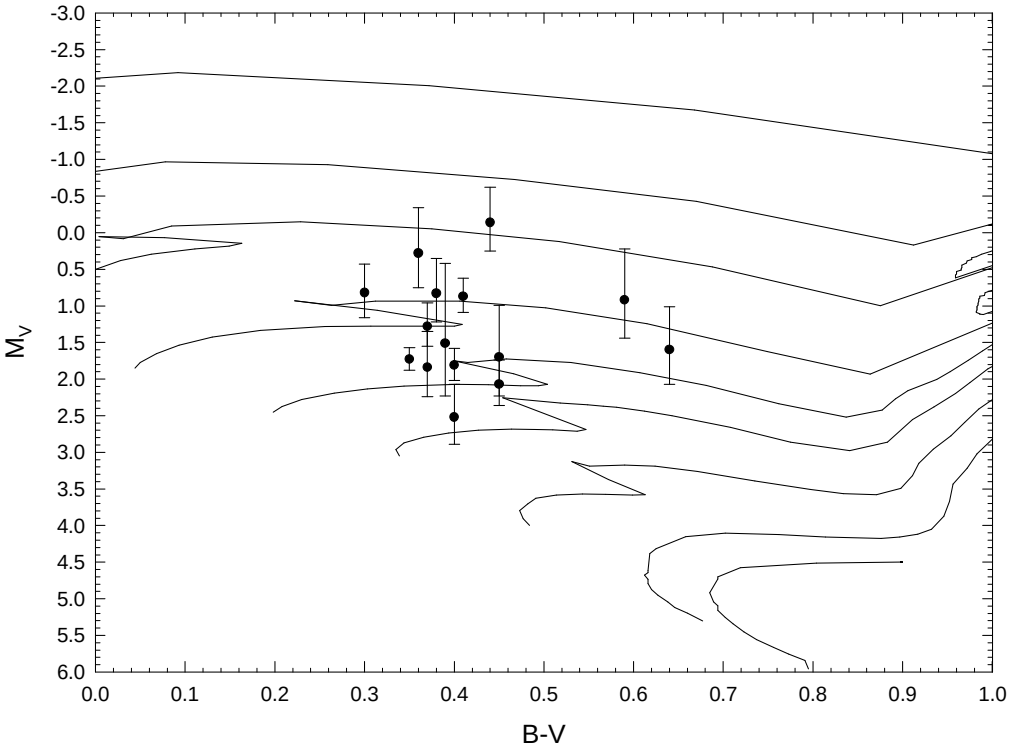

Figure 6.1 The resulting color-magnitude HR diagram for selected ρ Puppis stars. The "hooks" in the displayed evolutionary tracks (Lejeune & Schaerer, 2001) correspond to the phase of hydrogen exhaustion in the cores of the stars.

Upon inspection of the evolutionary state of the ρ Puppis stars, we see that most of these stars are near the point of hydrogen exhaustion. This is demonstrated in two HR diagrams, Figure 6.1, which is a color-absolute magnitude diagram and Figure 6.2, a temperature-gravity diagram. In both figures, theoretical evolutionary tracks are plotted (Lejeune & Schaerer 2001). Figure 6.1 depicts the evolutionary state for 16 of the ρ Puppis stars identified through spectral classification, based on the B-V color

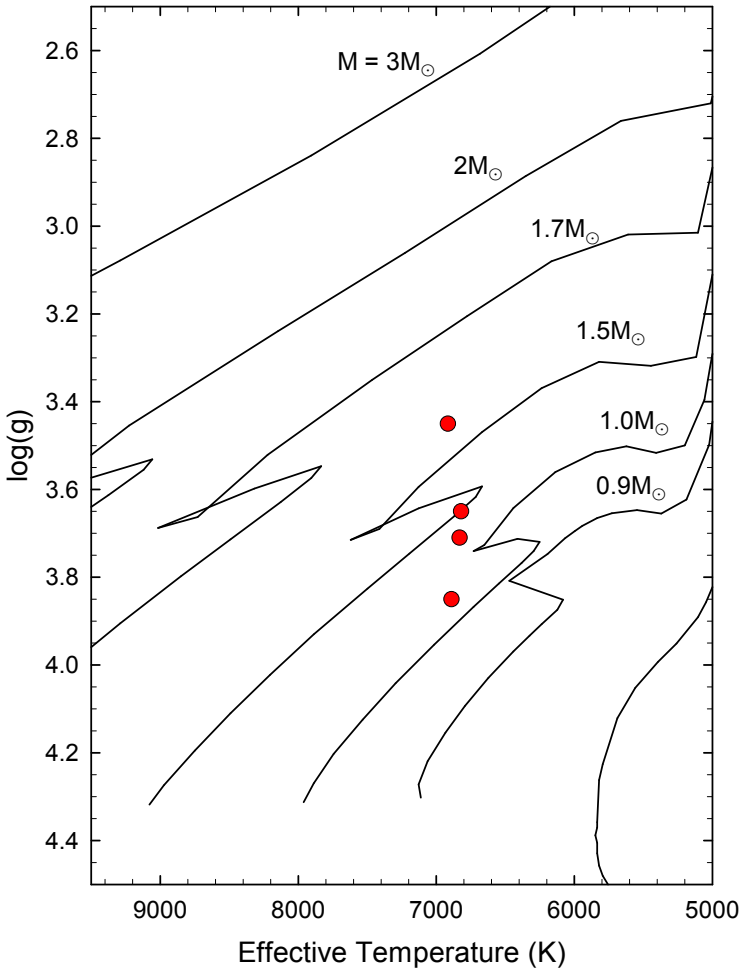

Figure 6.2 The resulting temperature-luminosity HR diagram for selected ρ Puppis stars.

and the absolute magnitude for each star. Figure 6.2 depicts the evolutionary state of the four ρ Puppis stars involved in the abundance analysis, in the $T_{\rm eff}$, $\log(g)$ plane. Both of these diagrams suggest that the ρ Puppis stars are at or near the terminal-age main sequence. This evolutionary state is associated with hydrogen exhaustion and the subsequent "hook" towards hotter temperatures, depicted in the evolutionary tracks in both HR diagrams.

This is interesting because it shows that there is a brief time, relatively speaking, at this evolutionary stage when the star will become hotter before it begins its rapid cooling and expansion period. This potentially means that Am stars could be cooling enough to re-establish He ionization and convection, but then, upon hydrogen exhaustion, they enter a phase of increased envelope temperatures, so that the convection is at least inhibited if not completely stopped. This could help to explain why we see a sudden drop in the number of Am stars at F2, and then a sharp peak coolward of F4, although this idea will need to be examined more closely through detailed modelling.

The time it takes for convection to completely erase the chemical peculiarities will be on the order of a few million years. This should be enough time in this rapid phase of evolution, for the star to achieve an effective temperature associated with an F5-type star while still maintaining the Am abundance peculiarities. The next obvious step in this project will be determining the timescales over which convection will be able to completely erase the chemical peculiarities of Am stars, so that we may determine more precisely where these stars are in their evolution.

Conclusions

The major results and conclusions of this thesis include (1) the discovery of 25 new ρ Puppis stars via spectral classification and (2) an abundance analysis of four ρ Puppis stars and the demonstration of enhanced abundances of Ba, Sr, and Eu, the latter an r-process element. This leads to the major conclusion that ρ Puppis stars are evolving Am stars, and did not obtain their chemical peculiarities via mass-transfer from an AGB companion.

Bibliography

Abt, H. A. 1961, ApJS, 6, 37

Adelman, S. J., Caliskan, H., Gulliver, A. F., & Teker, A. 2006, AA, 447, 685

Charbonneau, P. 1993, ASPC, 44, 474

Conti, P. S. 1969, ApJ, 158, 1085

Conti, P. S., & Strom, S. E. 1968, ApJ, 152, 483

Conti, P. S., & van den Heuvel, E. P. J. 1970, AA, 9, 466

Garrison, R. F. 1967, ApJ, 147, 1003

Glaspey, J. W. 1971, *The Upper Centaurus Association*, Ph.D. thesis, University of Arizona

Gray, R. O. 2009, *Documentation for Spectrum v2.76*, Appalachian State University

Gray, R. O., & Corbally, C. J. 2009, *Stellar Spectral Classification* (Princeton University Press)

Gray, R. O., & Corbally, C. J. 1994, AJ, 107, 742

Gray, R. O., Corbally, C. J., Garrison, R. F., McFadden, M. T., & Robinson, P. E. 2003, AJ, 126, 2048

Gray, R. O., & Garrison, R. F. 1989, ApJS, 69, 301

Gulliver, A. F., Hill, G., & Adelman, S. J. 1996, ASPC, 108, 232

Houk, N., & Smith-Moore, M. 1988, *Michigan Catalogue of Two-dimensional Spectral Types for the HD Stars. Volume 4, Declinations -26°.0 to -12°.0* (Ann Arbor, MI: University of Michigan Press)

Houk, N., & Swift, C. 1999, *Michigan catalogue of two-dimensional spectral types for the HD Stars; vol. 5* (Ann Arbor, MI: Department of Astronomy, University of Michigan)

Kreiken, E. A. 1935, ZA, 10, 199

Kurtz, D. W., Breger, M., Evans, S. W., & Sandmann, W. H. 1976, ApJ, 207, 181

Kurucz, R. 1993, ATLAS9 Stellar Atmosphere Programs and 2 km/s grid. Kurucz CD-ROM No. 13. Cambridge, Mass.: Smithsonian Astrophysical Observatory, 1993., 13

Lejeune, T., & Schaerer, D. 2001, AA, 366, 538

McClure, R. D. 1983, ApJ, 268, 264

Mermilliod, J-C., Mermilliod, M., & Hauck, B. 1997, A&AS, 124, 349

Michaud, G. 1970, ApJ, 160, 641

Morgan, W. W., Keenan, P. C., & Kellman, E. 1943, *An Atlas of Stellar Spectra* (Chicago, IL: University of Chicago Press)

Moultaka, J., Ilovaisky, S. A., Prugniel, P., & Soubiran, C. 2004, PASP, 116, 693

North, P., & Lanz, T. 1991, AA, 251, 489

Sbordone, L. 2005, Memorie della Societa Astronomica Italiana Supplement, 8, 61

Sbordone, L., Bonifacio, P., Castelli, F., & Kurucz, R. L. 2004, Memorie della Societa Astronomica Italiana Supplement, 5, 93

Slettebak, A. 1954, ApJ, 119, 146

Slettebak, A. 1955, ApJ, 121, 653

Smith, M. A. 1971, BAAS, 3, 11

Smith, M. A. 1973, ApJS, 25, 277

Stromgren, B. 1963, *Quantitative Classification Methods* (Chicago, IL: University of Chicago Press)

van den Heuvel, E. P. J. 1968, BAN, 19, 326

Warner, B. 1965, MNRAS, 129, 263

Watson, W. D. 1970, ApJ, 162L, 45

Watson, W. D. 1971, AA, 13, 263

Vita

Courtney Elizabeth McGahee was born in Greensboro, N.C. on 25 January 1981. She graduated from Southeast Guilford High School in June of 1999. She then attended the University of North Carolina at Wilmington for three semesters, after which she decided to transfer to Appalachian State University to focus her studies in Physics and Astronomy. In 2003 and 2004, Ms. McGahee became involved with NASA's NStars research under Dr. Richard O. Gray. In August 2004, Ms. McGahee received her Bachelor of Science in Applied Physics with a concentration in Astronomy and a Minor in Mathematics.

She then started her Master of Science in Engineering Physics at Appalachian State University in 2007. Ms. McGahee was awarded multiple observing runs at the Dominion Astrophysical Observatory of the Herzberg Institute of Astrophysics in Victoria, British Columbia, Canada to carry out her Master's research. She was also awarded a grant from Sigma Xi's Grants-In-Aid of Research program to cover travel expenses. Additional funding was obtained from a NASA Galex Space Telescope Grant.

After receiving her Master's in May 2010, Ms. McGahee accepted an offer from Clemson University to become a Graduate Assistant and begin her Doctorate of Philosophy in Physics.